THE CRYSTAL STRUCTURE OF RASPITE, $PbWO_4$

by

Diane Eileen Westfahl

1977

ProQuest LLC.
789 East Eisenhower Parkway
P.O. Box 1346
Ann Arbor, MI 48106 – 1346

T 1981

A thesis submitted to the Faculty and the Board of Trustees of the Colorado School of Mines in partial fulfillment of the requirements for the degree of Master of Science.

Signed: Diane Eileen Westfahl
Diane Eileen Westfahl

Golden, Colorado
Date: December 8, 1977

Approved:
Joseph J. Finney
Advisor

Joseph J. Finney
Head, Department of Geology

Golden, Colorado
Date: December 8, 1977

ABSTRACT

Raspite, $PbWO_4$, monoclinic, $P2_1/c$, a = 5.568, b = 4.978, c = 13.571 Å, $\beta = 107.68^{\circ}$, Z = 4, is one of the three known polymorphs of lead tungstate. The structure was solved by Patterson and difference syntheses. Least squares refinement converged to R = 0.092 for 630 unique reflections. Lead and tungsten positions were distinguishable on the basis of bond lengths only.

The structure consists of pairs of WO_4 tetrahedra separated from each other along {100} by lead atoms resulting in the perfect {100} cleavage. Average interatomic distances are: W - O, 1.9 Å and Pb - O, 2.64 Å. The structure shows strong similarities to the structures of both stolzite, the natural polymorph, and $PbWO_4$-III, the high temperature and pressure polymorph of lead tungstate.

TABLE OF CONTENTS

LIST OF ILLUSTRATIONS

LIST OF TABLES

INTRODUCTION

Occurrence and Physical Properties of Raspite

Raspite, $PbWO_4$, was first discovered in 1897 by C. Hlawatsch at the Proprietary Mine, Broken Hill, New South Wales, Australia. It was named after Mr. Rasp, the discoverer of this rich Ag, Pb, Zn deposit. There, raspite is found in cavities in "manganiferous oxidized vein material" (Dana, 1951) along with stolzite, a natural polymorph of $PbWO_4$ which is isostructural with scheelite (figure 3).

The Broken Hill district is one of the principal lead-silver-zinc producing areas in the world. Discovered in 1833, the deposit is contained in a thick series of metamorphosed Precambrian sediments. The principle ore zone consists of "two or more mineralized beds of contorted gneiss...distinguished by details of gangue mineralogy and metal ratios" (Park, MacDiarmid, 1970). The primary ore minerals are galena and sphalerite but the deposit is rich in other sulfides, sulfates, tungstates, antimonides, many of them rare and unusual. At the Broken Hill deposit, a gossan of quartz, limonite, manganese oxides and hematite originally extended to a depth of 300 feet. It is probable that raspite occurred in the gossan of the Broken Hill deposit. Raspite has also been reported in gold placers

of Soumidouro, Minas Geraes, Brazil, along with stolzite and scheelite; and in tin veins on the Cerro Estaño, east of Guanajuato, Mexico.

In color, raspite is light yellow, yellowish brown, or reportedly, gray. Its hardness is 2.5 to 3, with a density of 8.46 and an adamantine luster. Raspite exhibits a perfect {100} cleavage. Crystals are often tabular on {100} with this form elongated and striated parallel to [010] (figures 1 and 3). Less often, crystals are elongated along [100] or are thin and tabular on $\{\bar{1}01\}$. Raspite commonly twins on {100} (figures 1 and 3) and less commonly on $\{\bar{1}02\}$. The external morphology places raspite in class 2/m (Dana, 1951).

A chemical analysis follows:

	1	2
PbO	49.03	49.06
WO_3	50.97	48.32
Rem.	-	1.43
	100.00	98.81

1. $PbWO_4$. 2. Broken Hill, NSW.
Rem. is Fe_2O_3, MnO (in Dana, 1951).

The trace of manganese and iron oxides present in raspite may indicate a very slight amount of substitution for W.

Optically, raspite is biaxial (+) with a 2V nearly equal to zero. The refractive indices are:

Figure 1. Raspite crystals from Broken Hill, New South Wales, Australia. Length of large crystal is approximately 3 mm. Note twinned crystals in background. The raspite occurs on a matrix of manganese oxide bearing quartz with limonite.

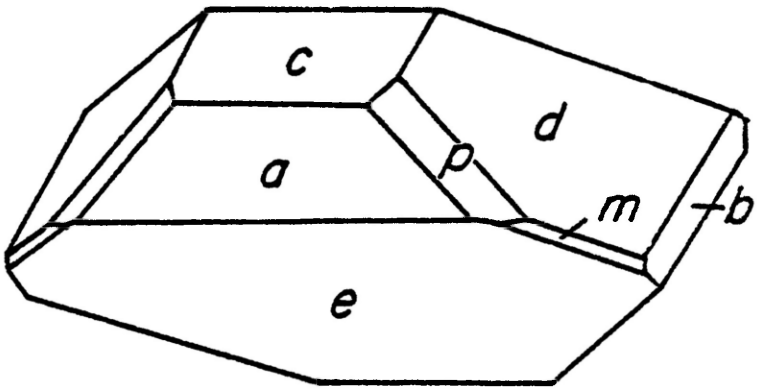

Figure 2. Drawing of raspite crystal from Minas Geraes, Brazil (Dana, 1951). c - {001}, b - {010}, a - {100}, m - {110}, d - {011}, e - {$\bar{1}$01}, p - {122}.

Figure 3. Twinned raspite (r) with stolzite (s) on manganese oxide bearing quartz with limonite from Broken Hill, New South Wales, Australia. Longest crystals are approximately 3 mm in length.

	N
X	2.27 ± .02
Y = b	2.27 ± .02
Z	2.30 ± .02
$Z \wedge c = 30^{o}$	(Dana, 1951)

The unit cell constants are:

$$a = 5.58\ \text{Å}$$

$$b = 5.00\ \text{Å}$$

$$c = 13.64\ \text{Å}$$

$$\beta = 107^{o}33'$$

and the space group is $P2_1/c$. The unit cell contains $Pb_4(WO_4)_4$ (Shaw and Claringbull, 1955).

Several studies of the chemistry of lead tungstate have been made: Jaeger and Gerns (1921), Jung (1931), both reported in Dana (1951); and Richter, Kruger and Pistorius (1976), but raspite has never been synthesized. Shaw and Claringbull reported that raspite transforms irreversibly to stolzite at about 400°C. The present study was undertaken in part because the raspite structure had not yet been solved and in part out of interest in possible structural similarities between raspite and stolzite as suggested by the raspite to stolzite transformation and the common occurrence of the two polymorphs together.

Acknowledgments

During the course of this study and in thesis work prior to this study, many people have provided invaluable assistance. Dr. Cortlandt Pierpont of the University of Colorado, Department of Chemistry authorized use of the facilities there for data collection and Curt Haltiwanger collected the data and offered many helpful suggestions during completion of the structure. Thanks are due to Dr. Joseph Finney, committee chairperson and advisor, for suggesting such fascinating minerals for study, for providing mineral specimens for use in this study, and for his encouragement throughout. The kind assistance of Dr. Subrata Ghose during data collection and initial work on a previous thesis project, and the discussions on direct methods with Dr. Alan Tench are also gratefully acknowledged. Color photographs of raspite crystals were provided by Webster Shipley.

EXPERIMENTAL

Crystal Selection

Raspite used in this study is from British Museum specimen B. M. 1972, 300, Raspite, Stolzite, NSW. In selecting a crystal for use in a structure determination, size and shape are important. The intensities of diffracted rays from a given crystal are proportional to the volume of the crystal. For this reason, the larger the crystal the better, within the limit that the crystal must be smaller than the cross-section of the x-ray beam. On the other hand, the larger the crystal, the greater the decrease in intensity of diffracted rays due to the effects of absorption. The linear absorption coefficient, μ_λ, is a good value by which to judge how large the effects of absorption will be for a given compound. Using this relation:

$$\mu_\lambda = \rho \sum_n (\text{wt } \%)(\mu/\rho_n)$$

the μ_λ calculated for raspite is 804 cm^{-1}. The calculation is reproduced in table 1. For comparison, an organic compound having no heavy atoms has a μ_λ value on the order of 10 cm^{-1}. Thus, for an organic compound having no heavy atoms, absorption can be ignored. However for raspite, the effect is extreme and care must be taken to minimize the problem of absorption. Selecting an appropriate size crystal is one way of minimizing absorption effects. There

Table 1. Calculation of the linear absorption coefficient, μ_λ, for raspite using Mo radiation. The mass absorption coefficients, μ/ρ, are taken from table 3.2.2A, Volume III, International Tables for X-Ray Crystallography.

	Atomic Weight	x	Atoms/Molecule		Weight Percent
Pb	207.9	x	1	= 207.9	207.9/455.7 = .46
W	183.8	x	1	= 183.8	183.8/455.7 = .40
O	16	x	4	= 64	64/455.7 = .14
				455.7	

	Weight Percent	x	μ/ρ cm^2/g	
Pb	.46	x	120	= 55.2
W	.40	x	99.1	= 39.64
O	.14	x	1.31	= .18
				95.04 cm^2/g = Σ wt % (μ/ρ)

$$\mu_\lambda = \rho(95.04)$$
$$= 8.46\ g/cm^3(95.04\ cm^2/g)$$
$$= 804\ cm^{-1}$$

exists for every compound a maximum crystal thickness for which the effects of absorption will not appear. Calculated by this expression:

$$t_{optimum} = \frac{2}{\mu\rho}$$

this thickness for raspite is 0.024 mm. Any crystal larger than this must be corrected for absorption. In practice, it is nearly impossible to cut such a small crystal. Even if such a crystal was obtained, counting times needed to record the very weak diffracted rays would make it impractical. Thus it is necessary to cut a very small crystal yet one large enough to produce readily measurable intensities. The raspite crystal used for data collection had an average radius of 0.063 mm.

Selecting a crystal with an appropriate shape can simplify the absorption corrections. Because incident and diffracted rays have different path lengths through the crystal for different reflections, different reflections will show the effects of absorption to a varying degree. This can be compensated for if the shape of the crystal is exactly known. Failing this, one may form the crystal into a convenient shape such as a cylinder or a sphere for which the absorption corrections can be routinely calculated. A sphere is the simplest shape to use because the correction depends only on the θ value for each reflection. Devices are available with which to grind spherical crystals

and this was attempted. Unfortunately, due to the perfect cleavage of raspite, efforts to form spheres resulted only in cleaving the crystals into many little flakes. As a last resort, crystals may be cut into roughly equidimensional fragments in the hope that the effects of absorption in such fragments do not differ significantly from those in a sphere. In this manner, spherical absorption corrections may be applied without introducing a particularly large error. The perfect, easy cleavage in raspite made it difficult to accomplish even this. The crystal finally chosen was not particularly equidimensional, the approximate ratio of the crystal's dimensions being 0.8:1.0:1.4. Thus, the spherical absorption corrections which were applied must be considered, at best, a crude approximation.

Precession Photography

Raspite commonly twins (figures 1 and 3) and it was necessary to take precession photographs of each crystal to determine whether or not it was twinned, and if so, to what extent. A crystal that is not twinned too severely may be used for data collection. In addition, precession photographs were used to confirm the unit cell and space group of raspite.

Each crystal was mounted on a glass fiber using a fast-hardening epoxy cement. The glass fibers were glued into

aluminum pins (figure 4) designed to fit into the goniometer head of a single crystal diffractometer. Each crystal was then aligned on the precession camera using a polaroid cassette. Using Mo Kα radiation, zero level precession photographs were taken of several crystals to determine the extent of twinning. A precession photograph of the twinned crystal used for data collection is shown in figure 5. The reflections from one member of the twin are considerably weaker than those from the other member of the twin, and appear clearly only after exposure times on the order of 70 hours. Except for reflections of class $0k\ell$, reflections from the two members of the twin do not fall on top of each other. Because of the separation of most of the reflections, it was hoped that the presence of the twin would not interfere with data collection. The pseudo mirror plane created by the twinning on {100} can be observed. Figure 6 shows an $h0\ell$ precession photograph of a much more extensively twinned crystal.

Unit cell constants were measured and found to be in agreement with the published ones. Z was calculated and the unit cell content was confirmed as $Pb_4(WO_4)_4$. The systematic absences observed confirm space group $P2_1/c$ with extinctions $h0\ell$: $\ell = 2n$; $0k0$: $k = 2n$. Representative precession photographs illustrating these extinctions are reproduced in figure 7.

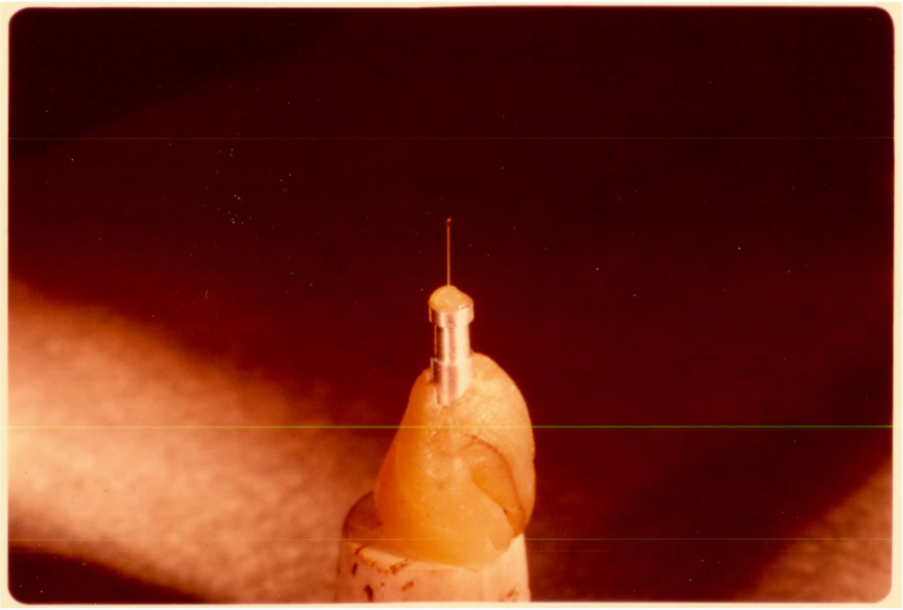

Figure 4. Raspite crystal mounted for data collection on a 4 mm long glass fiber.

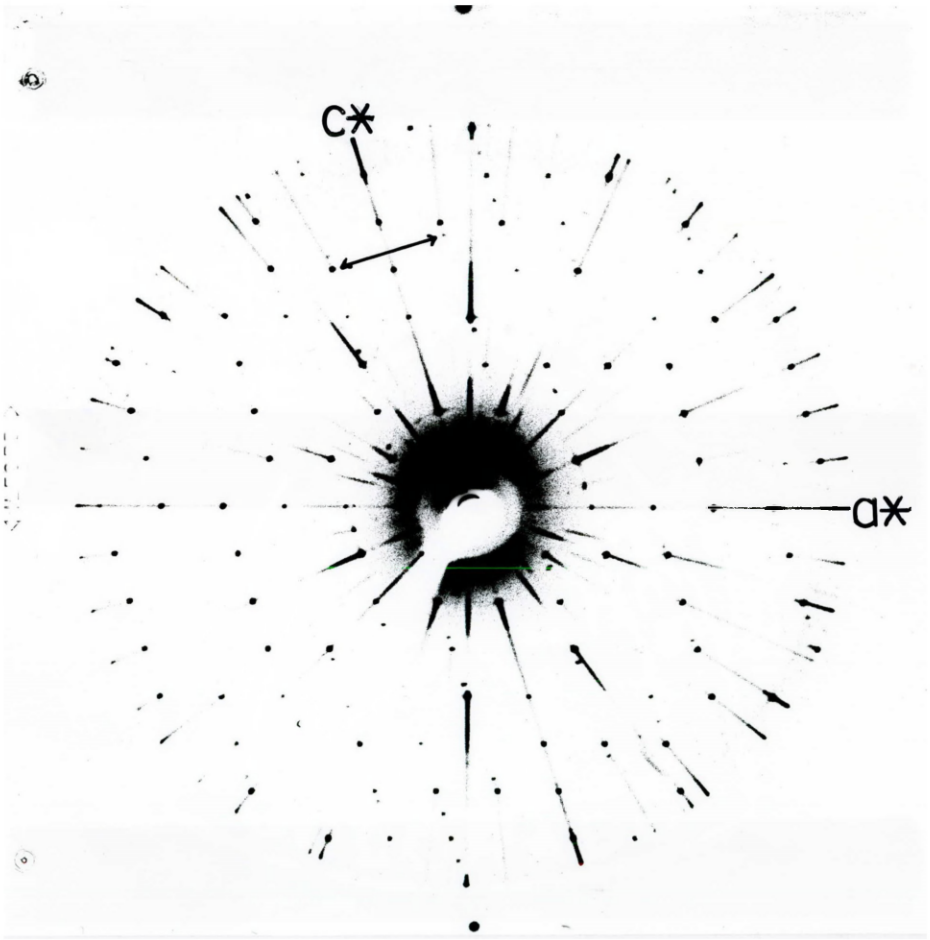

Figure 5. An h0ℓ precession photograph of the twinned raspite crystal used for data collection. Arrow connects one example of a pair of equivalent reflections, one from each member of the twin. Note the pseudo mirror plane along c* which separates the two equivalent reflections. 70 hours exposure using Mo Kα radiation with Zr filter at 40 KV and 20 ma.

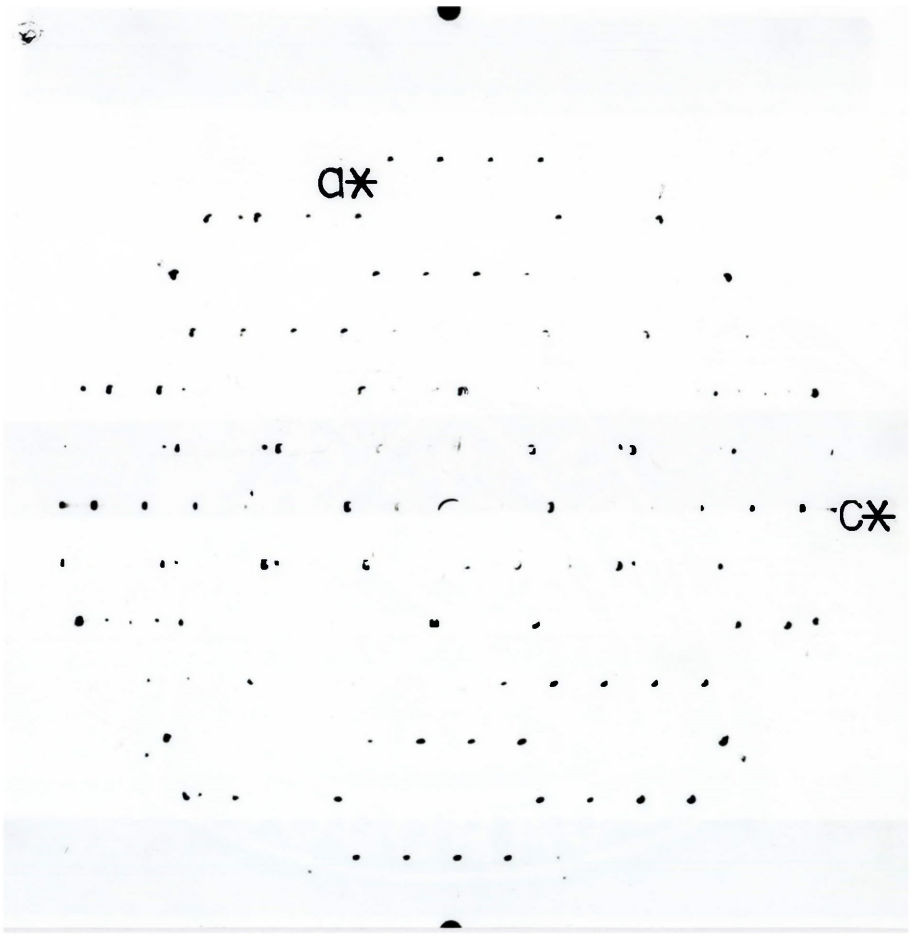

Figure 6. An h0ℓ precession photograph of an extensively twinned crystal: 24 hour exposure. "Doughnut" shaped spots are due to absorption effects. Pseudo mirror plane is horizontal along c*.

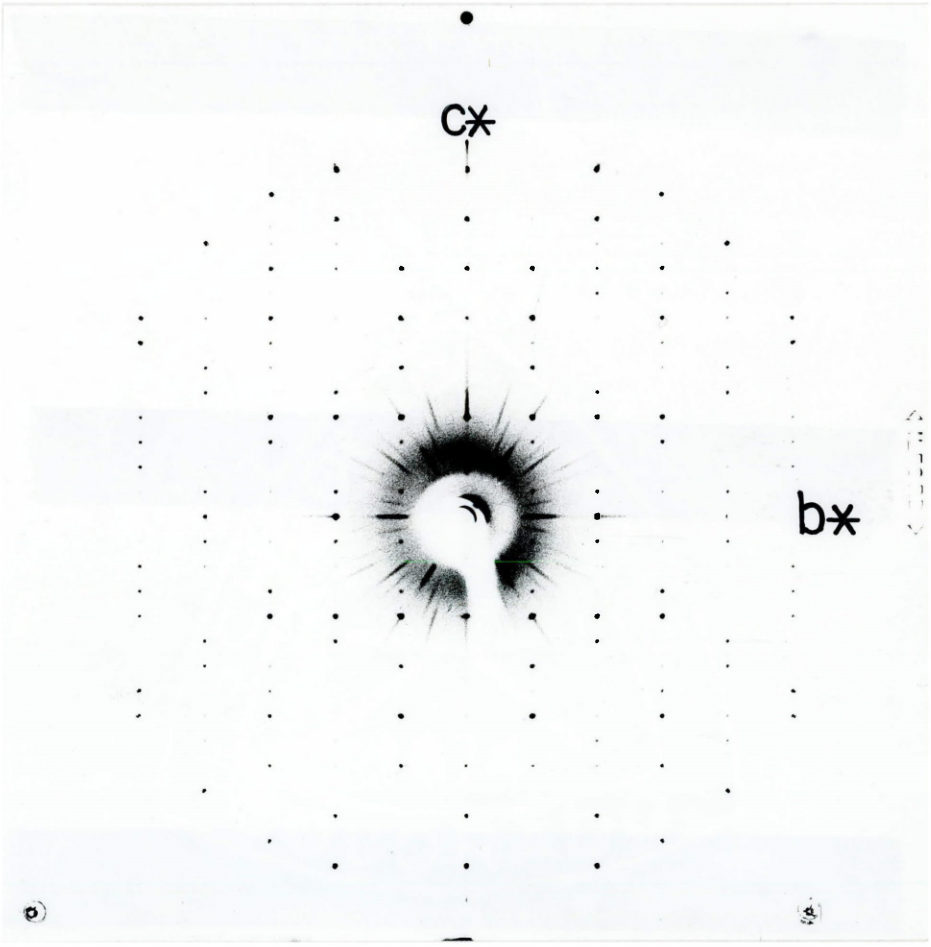

Figure 7a. A 0kℓ precession photograph with b* and c* labeled. 0k0 reflections are present where k = 2n.

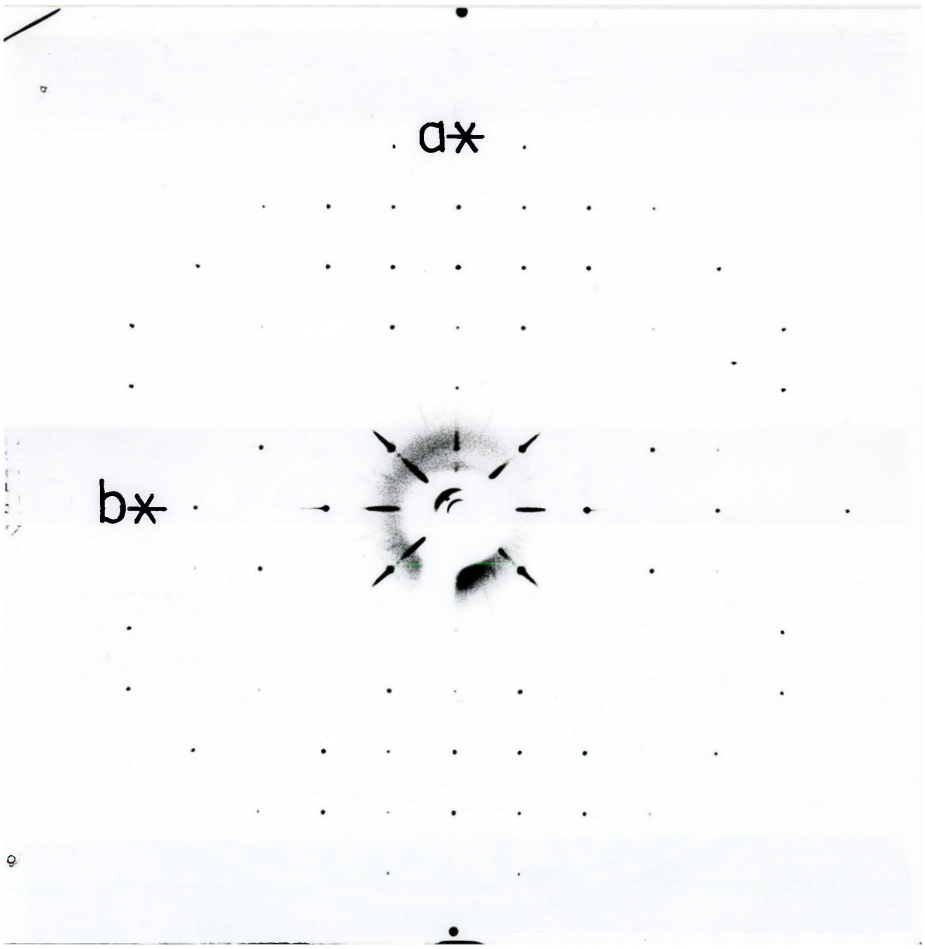

Figure 7b. An hk0 precession photograph with b* and a* labeled. 0k0 reflections are present where k = 2n.

Figure 7c. An hk1 precession photograph in same orientation as figure 7b. The hk1 reflections show no systematic absences.

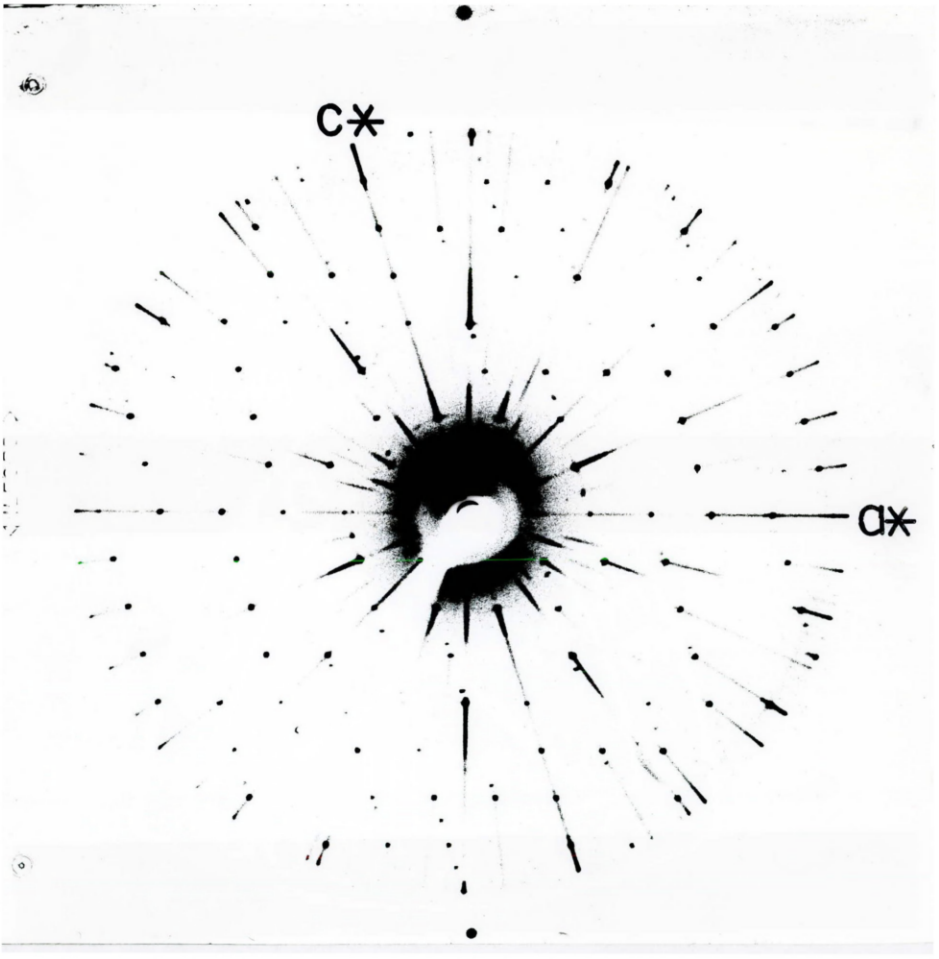

Figure 7d. An h0ℓ precession photograph with a* and c* labeled. The h0ℓ reflections are present where ℓ = 2n.

Data Collection

Data was collected on the Syntex P $\bar{1}$ auto-diffractometer in the Chemistry Department, University of Colorado, Boulder. Mo Kα radiation at 45 KV and 25 ma was used in conjunction with a graphite monochronometer. The θ - 2θ scan mode was used employing a constant scan rate of 1^{o}/min, scanning one degree on each side of each peak. Background was counted for thirty seconds on each side of each peak. Reflection data were collected up to 50^{o} 2θ over one quarter of the reciprocal sphere. Unit cell parameters were refined from twelve strong reflections. The refined cell constants are:

$a = 5.5683\ (14)\ \mathring{A}$ $\quad \alpha = 90.036\ (29)^{o}$

$b = 4.9783\ (13)\ \mathring{A}$ $\quad \beta = 107.678\ (22)^{o}$

$c = 13.5715\ (46)\ \mathring{A}$ $\quad \gamma = 90.018\ (21)^{o}$

$V = 358.45\ (17)\ \mathring{A}^{3}$

The refined cell constants are in good agreement with published parameters (Shaw and Claringbull, 1955). Data collection took approximately 45 hours at the end of which time 630 unique, non-extinct reflections had been measured. Four check reflections were remeasured at regular intervals during data collection. Raw data was output onto magnetic tape and also printed out on a teletype terminal during data collection.

Data Reduction

The raw intensity data was reduced using the computer program CUPBAR, a University of Colorado program designed to process the magnetic tape output by the Syntex P $\bar{1}$. This program accomplishes several things. It prints a plot for each check reflection of intensity versus time in order that intensity drift with time can be evaluated. It calculates a sigma value for each reflection for use in weighting reflections during structure refinement. The sigma value is calculated according to the relation

$$\sigma_I = [CT + .25(t_c/t_b)^2(B_1 + B_2) + (\rho I)^2]^{1/2}$$

where CT is the total integrated peak count obtained in time t_c, B_1 and B_2 are the background counts, each obtained in time t_b and $I = CT - .5\ (t_c/t_b)(B_1 + B_2)$. The value $(\rho I)^2$ is a "fudge" factor to prevent the assignment of excessively high weighting factors to strong reflections (Corfield, et al. 1967). Most importantly, the program takes the raw intensity data, $I_{(hkl)}$, and converts them into structure amplitudes or $F_{(hkl)}$ values. The relationship between $I_{(hkl)}$ and $F_{(hkl)}$ is

$$|F_{(hkl)}| = \sqrt{I_{(hkl)}/Lp}$$

where Lp is the correction for the Lorentz and polarization factors. The Lp corrections, for data collected on the Syntex P $\bar{1}$ with graphite monochronometer in perpendicular geometry, assuming the crystal to be 50% mosaic and 50%

perfect, are calculated according to the relation

$$Lp = \frac{1}{\sin 2\theta_c}\left[.5\left(\frac{\cos^2 2\theta_m + \cos^2 2\theta_c}{1 + \cos^2 2\theta_m}\right) + .5\left(\frac{\cos 2\theta_m + \cos^2 2\theta_c}{1 + \cos 2\theta_m}\right)\right]$$

where c refers to the crystal and m to the monochronometer.

Absorption corrections were postponed until the crystal had been measured and then were made using the program ABCOR adapted by the author from Colorado School of Mines program PREP1 for this purpose. This program calculates and applies spherical absorption corrections, given the average radius of the crystal and its μ_λ value, by interpolating between absorption correction factors for successive values of θ. The correction factors are taken from table 5.3.6B of Volume II of the International Tables for X-Ray Crystallography. Once the absorption corrections were made, the data were ready for use in solving the structure. A listing of $F_{(hkl)}$ observed values may be found in the appendix.

STRUCTURE DETERMINATION

Fourier Synthesis

Much of the mathematics of crystal structure analysis is based on the electron density Fourier series and its derivatives. A Fourier series may be used to approximate most periodic functions. The variation of electron density within a crystal is periodic. Thus the Fourier series representing the variation of electron density throughout a crystal is written:

$$\rho(XYZ) = \frac{1}{V_c} \sum_{-\infty}^{\infty} h \sum k \sum \ell \; F_{(hk\ell)} e^{-2\pi i(hX+kY+\ell Z)}.$$

The absolute value of the Fourier coefficient, $|F_{(hk\ell)}|$, is the quantity derived during data reduction, V_c is the volume of the unit cell, and X, Y, and Z are fractional coordinates of the unit cell. The sign or phase of the $F_{(hk\ell)}$ for each reflection is the unknown quantity in the electron density expression. No experimental method has yet been found for observing the phase of a reflection. Phases may only be calculated given the positions of the atoms. The inability to determine phases directly from observed $F_{(hk\ell)}$ values constitutes the "phase problem" of x-ray crystallography.

The Patterson function, which was employed in this study, is a Fourier series whose coefficient is $|F_{(hk\ell)}|^2$:

$$P(uvw) = \frac{1}{V_c^2} \Sigma h \Sigma k \Sigma \ell |F_{hk\ell}|^2 e^{2\pi i(hu+kv+\ell w)}.$$

Where, in the electron density synthesis, peaks represent concentrations of electrons or atom positions, peaks in the Patterson synthesis represent end points of vectors between atoms. For every set of atoms (x_1,y_1,z_1) and (x_2,y_2,z_2) in the electron density synthesis, there is a vector (u,v,w) in the Patterson synthesis, where $u = x_1 - x_2$, $v = y_1 - y_2$, and $w = z_1 - z_2$. If the Patterson summation is carried out for points at regular intervals throughout the unit cell of a crystal, a volume of vector densities is produced having the same dimensions as the unit cell. By algebraic manipulation of the positions of the maxima within this vector space, it is often possible to derive atom positions for at least the heavier atoms in the compound.

The Patterson summation is carried out by calculating vector densities at points in a grid along a series of parallel planes. The planes are parallel to some convenient crystallographic direction. The symmetry of the resulting Patterson map is the same as that of the space group less translational symmetry with the addition of a center at symmetry if one is not already present. For raspite, space group $P2_1/c$, the Patterson symmetry is 2/m. The presence of the mirror plane, m, made it necessary to calculate only half of the unit cell. A Patterson map was calculated for raspite using the Colorado School of Mines programs INPUT 2 and FOUR1.

Only those reflections having h, k, and ℓ values between plus and minus four were used to ensure a symmetric data set. The sampling interval or grid selected was approximately every 0.25 Å along all three axes. Sections were calculated at this interval from y equals zero to y equals one-half along the b axis, parallel to the a - c plane, {010}.

Patterson Map Interpretation

Space group $P2_1/c$ (figure 8) allows four two-fold special positions and one four-fold general position. All of the atoms in a unit cell of raspite can be placed into the general position set (e): one set containing four lead atoms, one containing four tungsten atoms, and four sets, each containing four oxygen atoms. The general form of vectors between atoms in the general position can be calculated by subtracting the four sets of coordinates of the position from each other. The Patterson vectors produced for space group $P2_1/c$ are:

	u,v,w
$x-\bar{x}$, $y-\bar{y}$, $z-\bar{z}$	= 2x,2y,2z
$x-\bar{x}$, $y-(1/2+y)$, $z-(1/2-z)$	= 2x,1/2,2z-1/2
x-x, $y-(1/2-y)$, $z-(1/2+z)$	= 0,2y-1/2,1/2

On the Patterson map of raspite, then, there should be concentrations of peaks on the section at v = 1/2, and along the line u = 0, w = 1/2, called the Harker section and line respectively, after David Harker, who first pointed out the

Monoclinic $2/m$ $P\,1\,2_1/c\,1$ No. 14 $P\,2_1/c$ C_{2h}^5

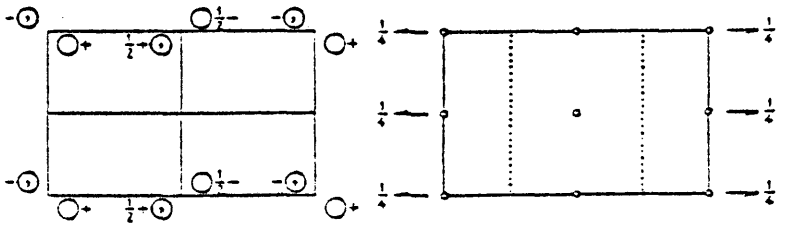

Origin at $\bar{1}$; unique axis b 2ND SETTING

Number of positions, Wyckoff notation, and point symmetry			Co-ordinates of equivalent positions	Conditions limiting possible reflections
				General:
4	e	1	x,y,z; $\bar{x},\bar{y},\bar{z}$; $\bar{x},\frac{1}{2}+y,\frac{1}{2}-z$; $x,\frac{1}{2}-y,\frac{1}{2}+z$.	hkl: No conditions $h0l$: $l=2n$ $0k0$: $k=2n$
				Special: as above, plus
2	d	$\bar{1}$	$\frac{1}{2},0,\frac{1}{2}$; $\frac{1}{2},\frac{1}{2},0$.	hkl: $k+l=2n$
2	c	$\bar{1}$	$0,0,\frac{1}{2}$; $0,\frac{1}{2},0$.	
2	b	$\bar{1}$	$\frac{1}{2},0,0$; $\frac{1}{2},\frac{1}{2},\frac{1}{2}$.	
2	a	$\bar{1}$	$0,0,0$; $0,\frac{1}{2},\frac{1}{2}$.	

Symmetry of special projections

(001) pgm; $a'=a$, $b'=b$ (100) pgg; $b'=b$, $c'=c$ (010) $p2$; $c'=c/2$, $a'=a$

Figure 8. Space group data - $P2_1/c$ from the International Tables for X-Ray Crystallography, Volume I.

usefulness of these symmetry-related concentrations of vectors (Buerger, 1959).

Once a Patterson map has been calculated, a search is made of the Harker section for Harker peaks likely to represent a vector between two crystallographically related atoms, such as a Pb - Pb vector. This type of peak is called an inversion peak if the atoms are related by a center of symmetry. The coordinates of a Harker peak on the Harker section for $P2_1/c$ are (2x,1/2,2z-1/2) and can be solved for x and z. To arrive at a y parameter, a search is made of the map for an inversion peak (2x,2y,2z) using the x and z just derived. If such a vector is present the y parameter is solved for, and the four crystallographically related atoms in one general position have been located. To find another atom, the same process is repeated using another set of inversion peaks, checking the resulting atoms by generating all the vectors between them and seeing if they are present on the Patterson map. Alternately a peak is selected representing a vector between atoms in two different general positions, one of which has already been located. The sum of the coordinates of the atom and such a vector should produce the coordinates of the other atom.

It is helpful during the initial steps in Patterson map interpretation to calculate the peak heights expected for vectors between the atom types present. The height of an

inversion peak is about equal to the square of the atomic number of the atom. The height of a vector between atoms in two different general positions is twice the product of the atomic numbers of the two atoms. The calculated values must be scaled to fit the height of the origin peak of the particular Patterson map. The peak heights expected on the Patterson map of raspite are shown calculated in table 2. Comparing the calculated peak heights, it is clear that inversion peaks are smaller than non-inversion peaks. Vectors between light atoms are much smaller than those between heavier ones. Thus, it is often difficult, especially if there are many atoms in the unit cell, to locate even the heavy atoms because the heavy atom inversion peaks may be obscured by larger non-inversion peaks. Light atoms are difficult to locate using a Patterson map in the presence of heavy atoms and other methods usually must be used.

The Patterson Map of Raspite

The Patterson map calculated for raspite was dominated by a few very large peaks. But, the peaks were all larger, by approximately one-third, than the calculated peak heights, complicating location of the inversion peaks. Because all the peaks were too large, the possibility existed that all of them were multiple peaks, several overlapping each other. Thus, even the largest peaks could contain inversion peaks.

Table 2. Calculation of expected peak heights for vectors on Patterson map of raspite.

Unit cell content = $Pb_4W_4O_{16}$

Origin peak height on map = 86461

$\sum_i Z_i^2$ = calculated origin peak height

$= 4(82^2) + 4(74^2) + 16(8^2)$

$= 49824$

Scale factor $= \frac{\text{observed origin height}}{\text{calculated origin height}}$

$= \frac{86461}{49824}$

$= 1.735$

		Expected Peak Heights
Pb - Pb inversion	$= (82^2)(1.735)$	= 11668
W - W inversion	$= (74^2)(1.735)$	= 9500
O - O inversion	$= (8^2)(1.735)$	= 222
Pb - W	$= 2(82)(74)(1.735)$	= 21055
Pb - O	$= 2(82)(8)(1.735)$	= 2276
W - O	$= 2(74)(8)(1.735)$	= 2054
O - O	$= 2(8^2)(1.735)$	= 444

In addition, all the peaks, without exception, were located either in the section at v = 0.0 or in the section at v = 0.5, the Harker section. These two sections are reproduced in figure 9.

The concentration of peaks on these two sections made the determination of the y coordinates for lead and tungsten routine. Remembering the general form of vectors (u,v,w) in this space group, the v parameters are either 2y,1/2, or 2y-1/2. The only values of y for which 2y and 2y-1/2 always equal 0.0 or 0.5 are .25 and .75. Either will work since by choosing one, the symmetry of the space group will generate atoms at the other. Finding the x and y coordinates for the two heavy atoms was equally straightforward. Because there was doubt as to which peaks on the Harker section were inversion peaks, a methodical trial of each peak was made. The parameters of each peak on the Harker section were solved for x and z. The resulting x and z coordinates were then combined with the parameters of the large peaks on the section at v = 0 which, it was hoped, represented Pb - W vectors. The atom positions produced were checked by generating all possible vectors between them and observing whether or not these vectors were present on the Patterson map. This process produced four separate solutions to the positions of the two heavy atoms, each of which accounted for all the vectors on the Patterson map. These solutions follow:

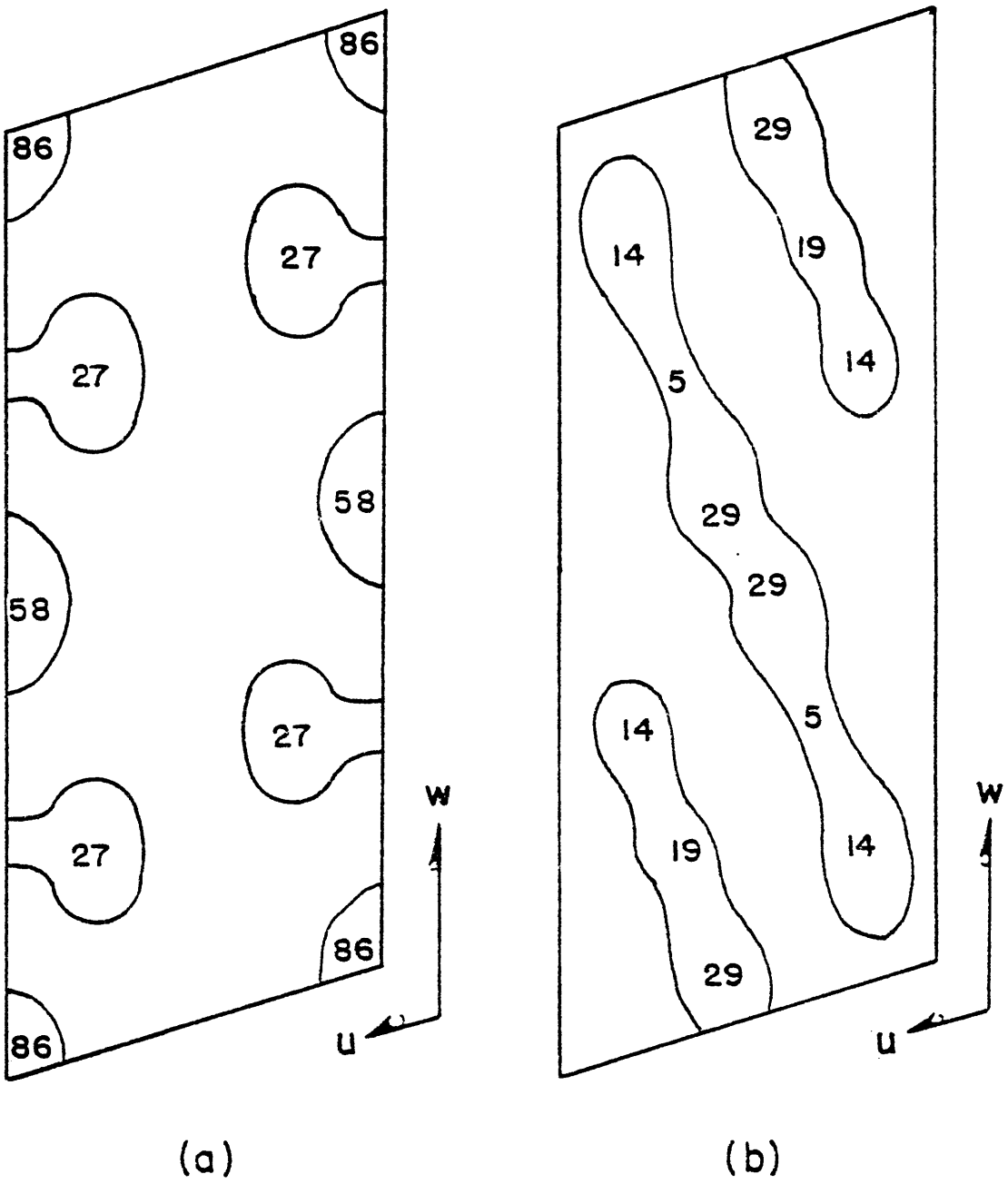

Figure 9. Patterson map of raspite. Sections at v = 0.0 (a) and v = 0.5 (b). Peak heights x 10^{-3}.

Solution Number	Atom 1			Atom 2		
	x	y	z	x	y	z
I	.33	.25	.10	.10	.25	.33
II	.38	.25	.17	.15	.25	.88
III	.10	.25	.08	.33	.25	.85
IV	.38	.25	.42	.16	.25	.14

STRUCTURE REFINEMENT

Structure Factor Calculation and Least Squares Refinement

To determine how correct the solutions were, each solution was subjected to three cycles of least squares refinement and structure factor calculations were made. A structure factor, $F_{(hk\ell)}$calc, may be calculated by the relation:

$$F_{(hk\ell)}\text{calc} = \Sigma f_n e^{2\pi i(hx_n+ky_n+\ell z_n)}$$

where f_i is the scattering factor of the n^{th} atom, (h,k,ℓ) are the Miller indices of the reflection, and x, y, and z are the coordinates of the atoms. The scattering factors were taken from Cromer and Mann (1968). Structure factor calculations produce a set of x-ray data equivalent to that generated if intensity data were to be collected from a compound possessing the proposed structure. Unlike the measured $F_{(hk\ell)}$ values, the $F_{(hk\ell)}$ values produced by structure factor calculations have phases which, if the proposed structure is correct, are also correct. The calculated phases are useful in later stages of structure refinement. The calculated set of data, $F_{(hk\ell)}$calc, is compared to the observed set, $F_{(hk\ell)}$obs, by calculating a residual index or R factor:

$$R = \frac{\Sigma\left||F_{obs}| - |F_{calc}|\right|}{\Sigma|F_{obs}|}$$

The value of the R factor is one indication of the correctness of a model. The more nearly identical the observed and

calculated data sets are, the smaller are the values of ΔF and R, and the more nearly correct the proposed structure is assumed to be.

The fortran program ORFLS (Busing, et al. 1962) was used for refinement and structure factor calculations. ORFLS performs successive cycles of least-squares refinement minimizing the expression $\Sigma(|F_{obs}| - |F_{calc}|)$ using the full matrix of normal equations. Following each cycle, a list of F_{obs} and F_{calc} values is output along with the R factor for that cycle. After the final cycle, a correlation matrix is computed. In the initial refinement, only the scale factor and the atomic coordinates of the lead and tungsten were allowed to vary. The final R for each solution follows:

I	R = 0.45
II	R = 0.43
III	R = 0.27
IV	R = 0.27

Because of their higher R values, the first two solutions were discarded and one of the second two was arbitrarily selected for further refinement. It was noted that solution IV can be derived from III and solution II from I, by shifting the origin by (1/2,1/2,1/2). Solution IV was chosen for further refinement. The atom coordinates of this model output by ORFLS after the initial three cycles of refinement were:

Atom 1	Atom 2
x = .387	x = .166
y = .250	y = .195
z = .422	z = .149

With the exception of the y coordinate of atom 2, these positions were unchanged from those derived from the Patterson map. At this stage it was still impossible to distinguish which position contained lead and which tungsten. The refinement was attempted both ways with the results inconclusive. With atom 1 as lead, R = 0.273 and with atom 2 as lead, R = 0.271. The second structure was selected for use merely on the basis of the slightly lower R.

ΔF Synthesis

Locating light atoms in the presence of heavier ones is often difficult. This difficulty becomes extreme when, as in raspite, it is the positions of oxygen atoms, atomic number eight, that are being sought in the presence of lead and tungsten. Finding the oxygen positions of raspite was the longest and most trying part of this study. Considering that of the many ABO_4 type compounds containing heavy atoms, fewer than half have had oxygen locations successfully determined, this is not surprising. The method employed in locating these atoms was the ΔF synthesis. Written in this form:

$$\Delta\rho = \rho_{obs} - \rho_{calc} = \frac{1}{V} \Sigma h \Sigma k \Sigma \ell (F_{obs} - F_{calc}) e^{-2\pi i(hX+kY+\ell Z)},$$

the ΔF synthesis is a Fourier series, the coefficient of which is $(F_{obs}-F_{calc})$ or ΔF. The difference Fourier synthesis uses the F_{obs} and F_{calc} values output by the least squares refinement and structure factor calculation process, with the phase of F_{calc} assigned to F_{obs}. The ΔF synthesis produces a three-dimensional map which contains useful information about errors in position and temperature coefficients of atoms already located, and positions of atoms not yet in the structure. Like the Patterson map, the ΔF, or difference map, is calculated in sections and printed by the computer. Two different sets of programs were used to calculate difference maps: INPUT2 and FOUR1, and NRC2 and NRC8 (Ahmed, et al. 1967). The two sets produced similar maps.

Difference maps were computed using F_{obs} and F_{calc} values produced during the last cycle of refinement of solution IV. The maps produced contained many peaks which appeared likely to represent oxygen positions. Theoretically, if a correct atom position is added to a structure, and the structure is refined for a few cycles, the R factor should be reduced. However, when this was attempted with potential oxygen positions taken from the difference maps, the results were inconclusive. Some of the trial oxygen positions when added to the structure caused the R to increase and were discarded as incorrect. Others caused the R factor to

decrease but only by a fraction of a percent, certainly not a large enough change to be significant and indicate a correct position. None of the positions caused a decrease in R by as much as a half percent. Models of the structure were constructed in an attempt to determine, based on packing and space considerations, where the oxygen atoms might be. Finally, it was suggested that the temperature coefficients of the lead and tungsten be allowed to refine. The temperature coefficients represent the vibration of the atoms in the structure. This tactic has been used successfully in locating light atoms in organo-metallic compounds. Several cycles of refinement were run, allowing the temperature coefficients to vary and the R factor dropped immediately to 0.14.

A new difference map was calculated using output from the last refinement cycle. This map was somewhat different from the earlier maps. Because of the lower R factor and ΔF values, the peak heights on the map were all lower. Also, while the locations of the peaks and valleys on the map were unchanged, peaks on the old map now appeared as valleys, and valleys were now peaks. The reversal of peaks and valleys reflects the considerable increase in size of the thermal coefficients during refinement. Valleys on the new map represented correct oxygen positions. As before, refining an incorrect position caused the R factor to

increase and either its temperature factor to become very large or the position itself to drift. Correct oxygen positions did not move much during refinement and caused the R factor to decrease by approximately 0.01. This is not an extremely large change but a decrease of 0.01 at an R of 0.14 is a much larger relative change than anything that had been observed up to this point.

In the final stages of oxygen atom location, the lead and tungsten positions were interchanged several times in the hope that it would become obvious which site contained which heavy atom. Interchanging the positions caused neither the R to change nor the oxygen positions to shift. The bond lengths were the most reasonable for the configuration finally chosen and it was solely on the basis of bond lengths that the identities of the heavy atom positions were established. Refinement had, by this time, reduced the R to 0.103.

Accurate bond lengths and angles needed to be calculated for use in describing the structure and comparing it with other similar structures. The program BLENG, a Colorado School of Mines program, was used for this purpose. The results were not encouraging. While the average bond lengths were comparable to bond lengths in other similar compounds, many specific bond lengths were not. Attempts were made to shift some of the oxygens slightly into positions which would result in more acceptable bond lengths. These attempts

failed. Either the oxygen atom in question would refine to its original position or its temperature coefficient would become very large. No improvement was achieved and so the oxygens were left in the positions to which they originally refined.

After abandoning attempts to improve bond lengths, final cycles of refinement were run, converting isotropic temperature coefficients to anisotropic ones. Isotropic temperature coefficients, which had been used up to this point, assume that the atom is vibrating uniformly in all directions. Anisotropic temperature coefficients assume the atom is vibrating more irregularly and are closer to representing reality. Attempts to refine anisotropic temperature coefficients for the oxygen positions were unsuccessful in that the temperature coefficients for oxygens 1, 2, and 4 became negative during refinement. The reason for this is not definite but may have something to do with the peculiar bond lengths displayed by the structure. In the final refinement cycles, anisotropic temperature coefficients were refined for the lead and tungsten atoms only, and the R dropped to 0.092. A listing of the final F_{obs} and F_{calc} values may be found in the appendix.

Intermittently during refinement, the calculations were carried out using weighting factors for each reflection based on the sigma values derived during data reduction. The

weighting factor input into ORFLS is derived from that calculated during data reduction by the expression

$$\sigma = \frac{1}{2} \frac{\sigma_I}{F_{obs}} ,$$

allowing more weight to those reflections measured with the greatest accuracy. This sometimes results in a lower R factor but in this case, the weighted R factor was always several percent greater than the R calculated with each reflection given a weight of unity. Weighting factors were not used in the final calculations.

DISCUSSION OF THE STRUCTURE

Description

The final atomic coordinates and thermal parameters are listed in table 3. Bond lengths and angles around tungsten and lead are listed in table 4. The structure consists of pairs of distorted WO_4 tetrahedra separated from each other along {100} by lead atoms. The concentration of lead atoms along {100} results in raspites' perfect cleavage. The pairs of WO_4 tetrahedra are most apparent when viewed down the b axis as in figure 10. Within each pair of tetrahedra, one oxygen of each tetrahedron is close enough to the tungsten of the other tetrahedron in the pair to be considered shared by both. A five-fold coordination of oxygens around each tungsten is produced with an average W - O distance of 1.9 Å. Figure 13 illustrates the bond lengths, angles, and coordination in a tungsten - oxygen tetrahedra pair. There are seven oxygen atoms around each lead atom, five at an average distance of 2.44 Å and two more at a distance of 3.16 Å. The average Pb - O distance is 2.64 Å which is comparable to Pb - O distances in other compounds.

In both figures 10 and 12, the vibration directions of the refractive indices have been indicated. The vibration directions clearly parallel those directions in the structure in which there is the most "open space". They also parallel

Table 3. Fractional coordinates and thermal parameters.

	x	y	z
Pb	.1664(4)	.1922(5)	.1496(2)
W	.3885(4)	.2492(5)	.4228(2)
01	.5439(80)	.8806(98)	.1746(33)
02	.7194(66)	.4546(82)	.5165(27)
03	.1002(87)	.1267(107)	.3431(35)
04	.3980(66)	.4293(81)	.0605(27)

	β_{11} or B, $\AA^2$	β_{22}	β_{33}	β_{12}	β_{13}	β_{23}
Pb	.02884(93)	.03190(116)	.00523(16)	-.00046(80)	.00306(29)	.00006(33)
W	.02511(93)	.02485(112)	.00438(15)	-.00037(74)	.00194(28)	-.00013(33)
01	3.88(1.00)					
02	2.76(76)					
03	4.25(82)					
04	2.54(72)					

Table 4. Bond lengths and angles around Pb and W.

W - O		O - W - O Angles		
	W	02	03	04
01	1.42(08)Å	90.35°	72.97°	117.59°
02	1.70(07)		105.27°	138.77°
03	2.27(08)			111.42°
04	2.04(06)	Avg	106.06°	
04	2.08(06)			
Avg	1.9 Å			

Pb - O	
	Pb
01	2.72(08)Å
02	2.45(07)
02	3.15(07)
03	2.56(09)
03	2.61(09)
03	3.17(09)
04	1.89(07)
Avg	2.64 Å

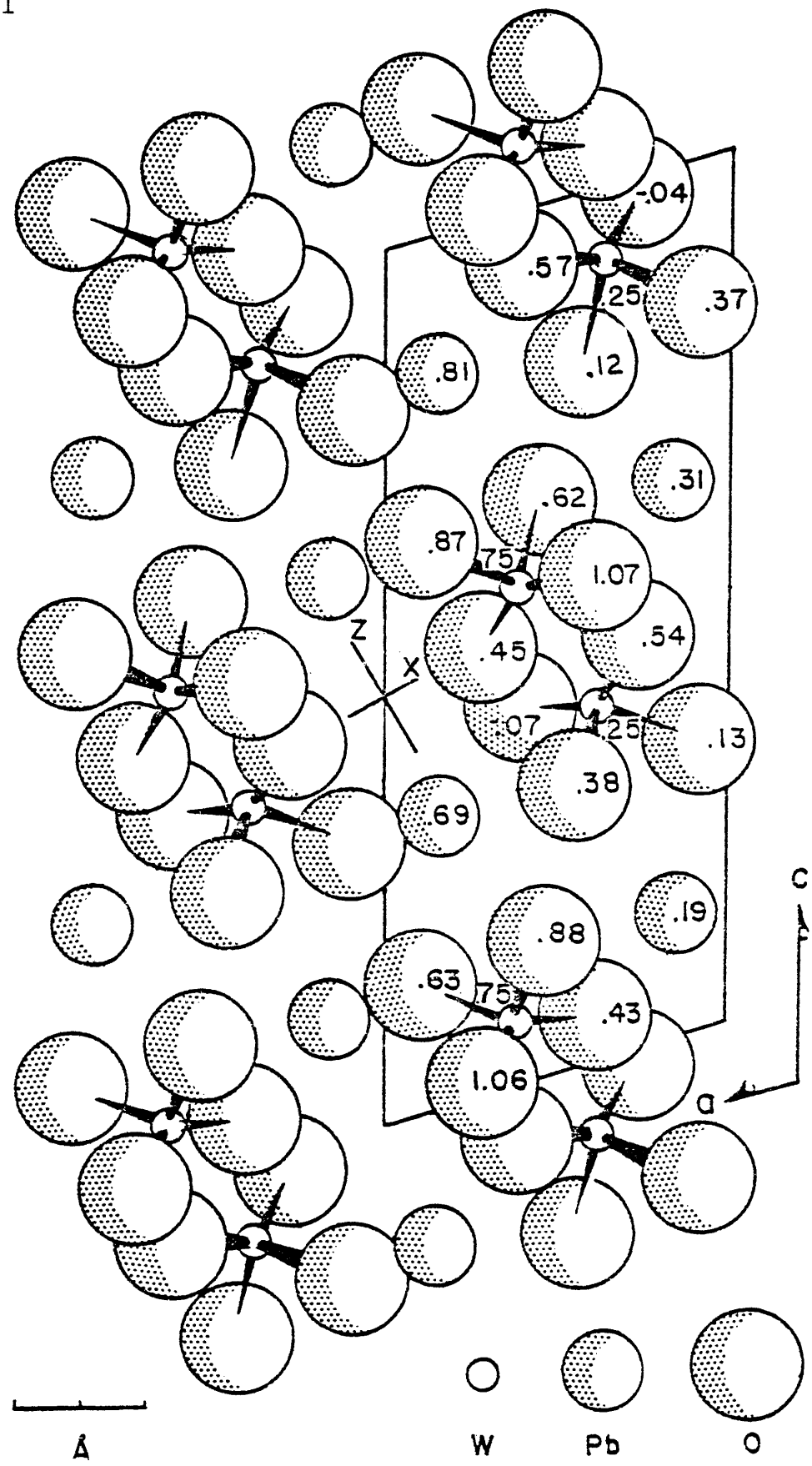

Figure 10. Raspite structure projected on {010}. Numbers represent the *y* coordinates of the atoms.

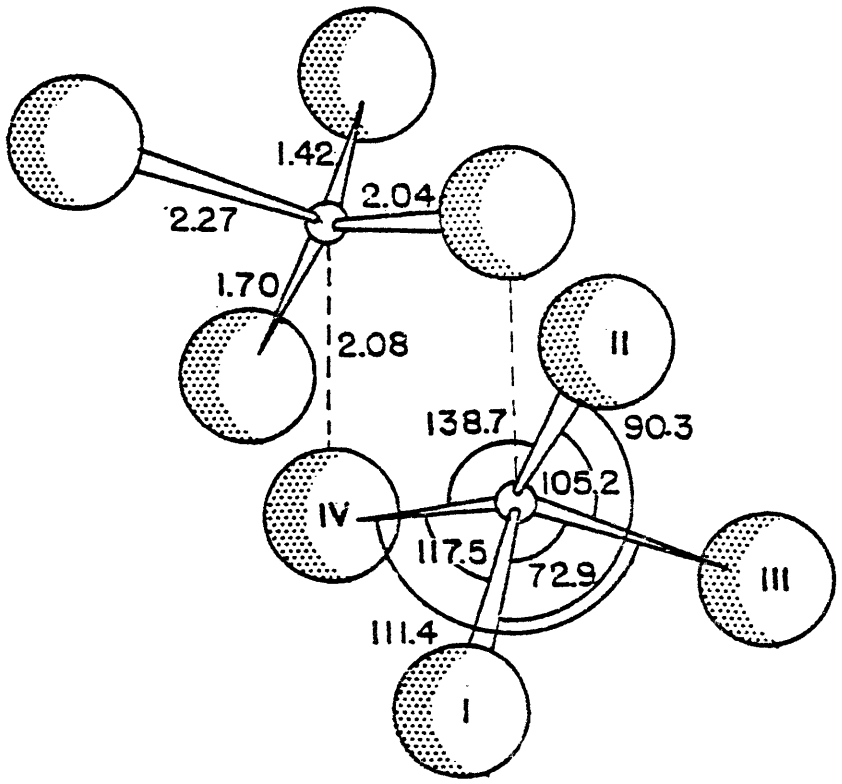

Figure 11. WO_4 tetrahedral pair showing bond lengths (Å) and angles (degrees). Dotted line indicates oxygens shared by both tetrahedra.

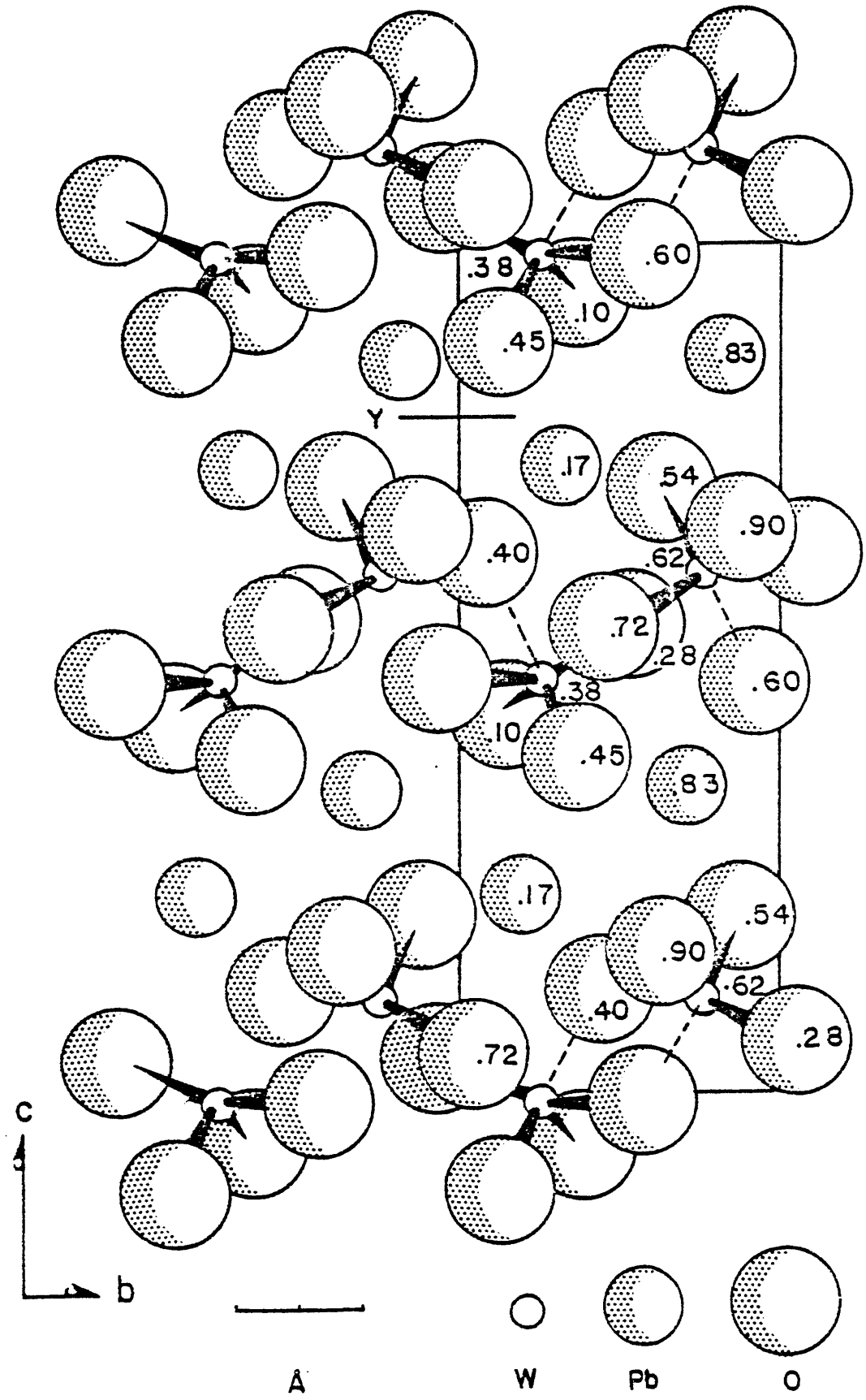

Figure 12. Raspite structure projected on {100}. Dotted lines connect oxygens shared by both tetrahedra of a pair. Numbers represent x coordinates of the atoms.

the edges of the oxygen tetrahedra. It appears in figure 12 that the coordination of oxygen around tungsten is approaching octahedral with nearby octahedra sharing edges. These linked octahedra form infinite chains paralleling the b axis.

Sources of Error

It is apparent when examining the calculated bond lengths that while the average values are acceptable, individual bond lengths deviate significantly from expected average values. The shorter bond lengths are physically unlikely, if not impossible. It appears that while the general arrangement of oxygen atoms is probably correct, individual positions have not refined well, resulting in these peculiar bond lengths.

There are two factors in the data which may contribute to this situation. Spherical absorption corrections were applied to data collected from a non-spherical crystal. This undoubtedly introduced a systematic error in the observed data which may be reflected in the way all the positions have refined. Because lead and tungsten account for 83 percent of the scattering in raspite, very small changes in positions of the heavy atoms could cause errors in the oxygen positions.

The other factor which may be contributing to error is anomalous dispersion. Anomalous dispersion occurs when the

wavelength of radiation used falls near an absorption edge of an element being irradiated. An anomalous phase change occurs during scattering by the electrons associated with that particular absorption edge. Since data was collected using Mo radiation, there is no doubt that the lead and tungsten behaved in this fashion. The effect causes the scattering factor for each atom which is anomalously dispersing to be a complex quantity:

$$f_o^{anom} = f_o + \Delta f' + i\Delta f''$$

where f_o is the normal scattering factor, $\Delta f'$, a real correction term, and $\Delta f''$, the imaginary component. The program used for structure factor calculation, ORFLS, does not have the capability of calculating or applying these correction terms. For this reason the F_{calc} values were not corrected for anomalous dispersion. In practice, anomalous dispersion is said to manifest itself by making elements behave as if they were heavier than they actually are. This may explain why the peaks on the Patterson map were all too large. Also, it might explain why adding the oxygen atoms to the structure, which comprise 17 percent of the total scattering, resulted in such a small decrease in R. Using F_{calc} values for refinement which were not corrected for this probably did not have a positive effect on the accuracy of the final positions.

In view of these sources of error in the observed and calculated data, it may be that in raspite, the WO_4 tetrahedra are somewhat less distorted than they appear here to be. A considerable amount of distortion is reasonable however. It is a fact that in the isostructural series of tungstates comprising the wolframite group, the larger the cation, the more distorted is the surrounding coordination polyhedron of oxygen atoms (Weitzel, 1976). Lead, with an ionic radius of 1.2 Å is too large to fit into the wolframite structure which accommodates cations with radii less than 0.98 Å. Yet the structure of raspite is enough like that of the wolframite group for this trend to be valid, the raspite structure showing an extreme example of this distortion.

Comparison with Stolzite and $PbWO_4$-III

Another structure which is similar to that of raspite is the scheelite structure. The other natural polymorph of lead tungstate, stolzite, crystallizes into this structure. Stolzite is very like raspite. Physically, it has the same color and hardness. Its specific gravity, 7.9-8.3, and refractive indices, $\omega = 2.27$, $\varepsilon = 2.19$, are slightly lower and it has a somewhat less brilliant luster (Dana, 1951). The unit cell is tetragonal, space group $I4_1/a$ with cell constants $a = 5.45$ Å, $c = 12.02$ Å. The unit cell shape and volume, 355.4 $Å^3$, are almost identical to that of raspite

and the cell content is the same (Wycoff, 1965). As can be seen in figure 13, the basic building unit of stolzite, as in raspite, is pairs of WO_4 tetrahedra separated from each other by lead atoms. The tetrahedra are flattened perpendicular to the c axis but otherwise are very regular. The coordination of oxygen around tungsten is four-fold with the W - O distance equal to 1.78 Å. The combination of both lower coordination and shorter bond lengths than observed in raspite probably results in a fairly similar charge distribution around the tungsten in the two minerals. The lead atoms in stolzite are each surrounded by eight oxygen atoms, four at a distance of 2.59 Å and four more at a distance of 3.21 Å resulting in an average Pb - O distance of 2.9 Å. Even though the coordination around lead is slightly higher than that in raspite, the fact that the average Pb - O distance in stolzite is .25 Å longer than in raspite undoubtedly accounts for the slightly lower density observed in stolzite as compared to raspite.

Comparing the structures of these two minerals, it is not difficult to envision the transformation from raspite to stolzite. The raspite structure, irregular as it is, is merely a contorted version of stolzite. This is illustrated in figure 14 where the distorted "stolzite" unit cell has been outlined on the raspite structure. Other than the fact that the y coordinates of the two "middle" tetrahedra have

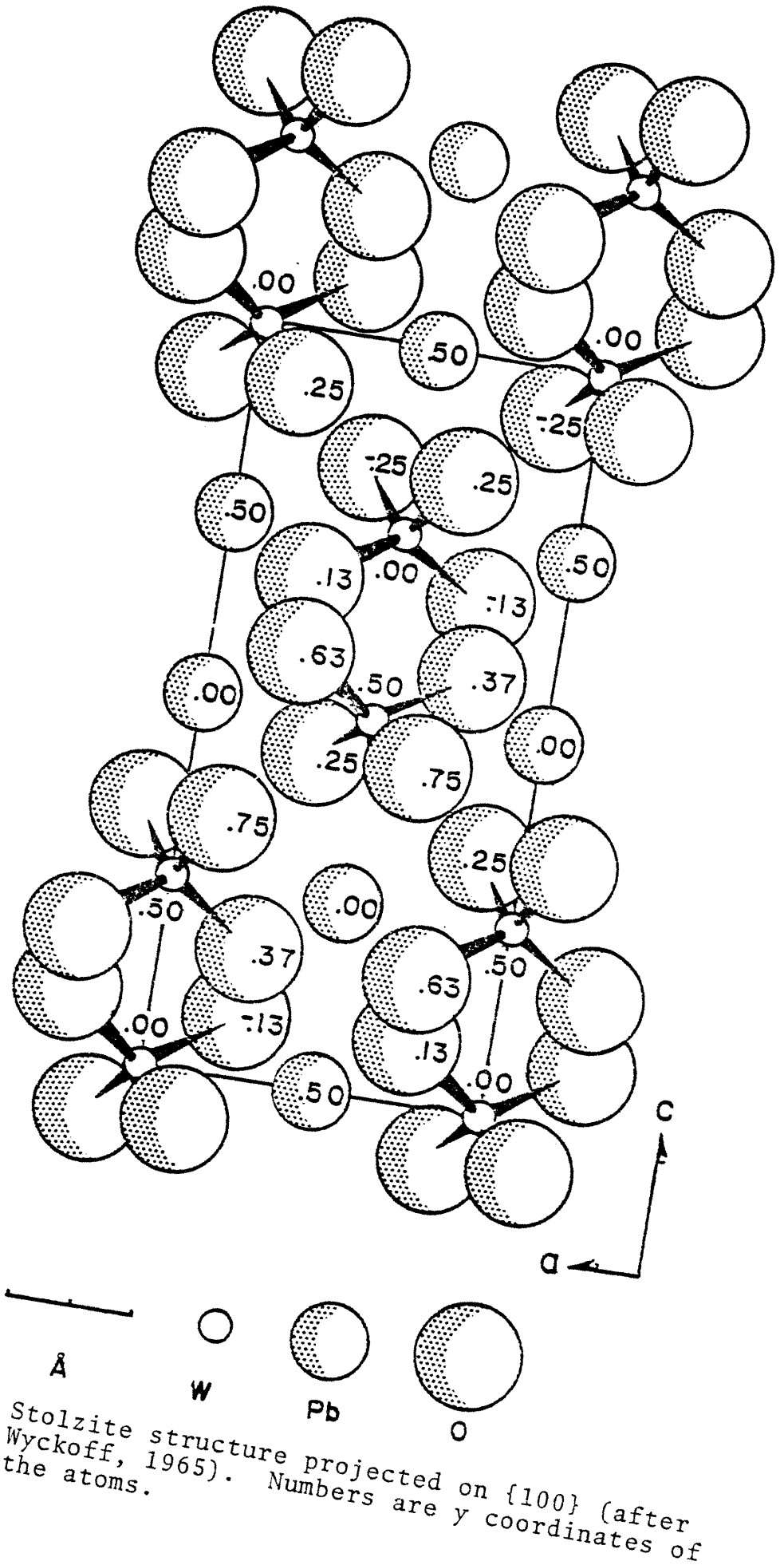

Figure 13. Stolzite structure projected on {100} (after Wyckoff, 1965). Numbers are y coordinates of the atoms.

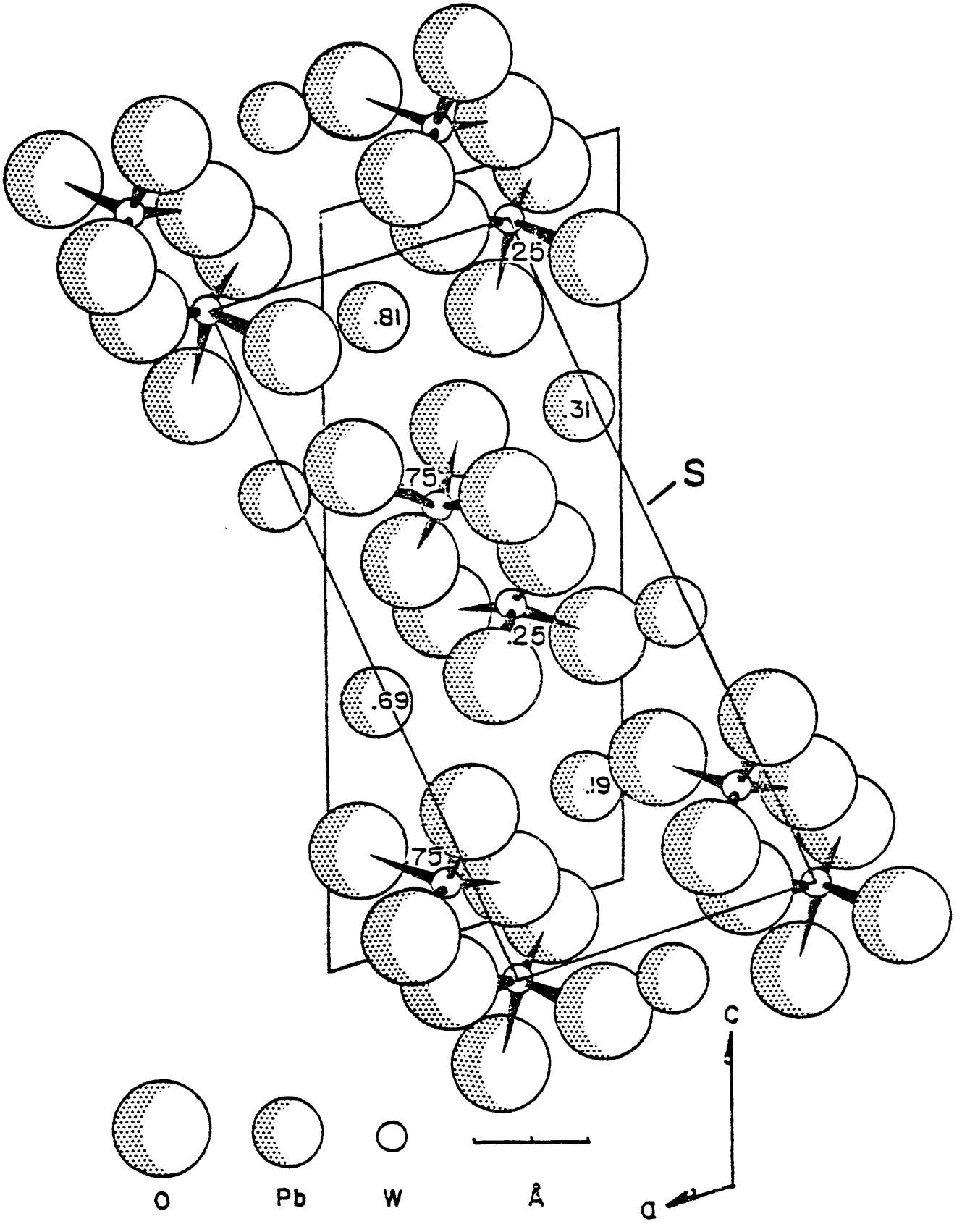

Figure 14. Raspite structure, {010} projection, showing distorted stolzite cell (S). Numbers represent y coordinates of lead and tungsten. See figure 10 for y coordinates of oxygen.

been reversed the positions are all analogous. At approximately 400°C, the increased thermal vibration of the atoms probably exceeds the strength of the contorted raspite lattice and the structure literally shakes itself apart, settling into the more regular structure of stolzite. This transformation is accomplished by no more than slight rotations of tetrahedra and realignments of the heavy atoms into the higher symmetry of stolzite's body-centered tetragonal cell.

The third lead tungstate polymorph, $PbWO_4$-III, is prepared by holding stolzite at 500°C and 32 kbar for four hours and then cooling it slowly before releasing the pressure. $PbWO_4$-III, density 9.19 gm/cm^3, is isostructural with high temperature $BaWO_4$ which is the most densely packed ABO_4 type phase known. A drawing of the $PbWO_4$-III structure, space group $P2_1/n$, is reproduced in figure 15 and the associated bond lengths and angles may be found in table 5 (Richter, Kruger, and Pistorius, 1976). In the $PbWO_4$-III structure, the tungsten is octahedrally coordinated with three oxygen atoms approximately 1.8 Å away and three more 2.1 Å away with the average W - O distance being 1.95 Å. The tungsten - oxygen octahedra share edges and corners forming sheets perpendicular to the a axis. Comparing this arrangement with the raspite structure, {100} projection (figure 12), some general similarities appear. Viewed from

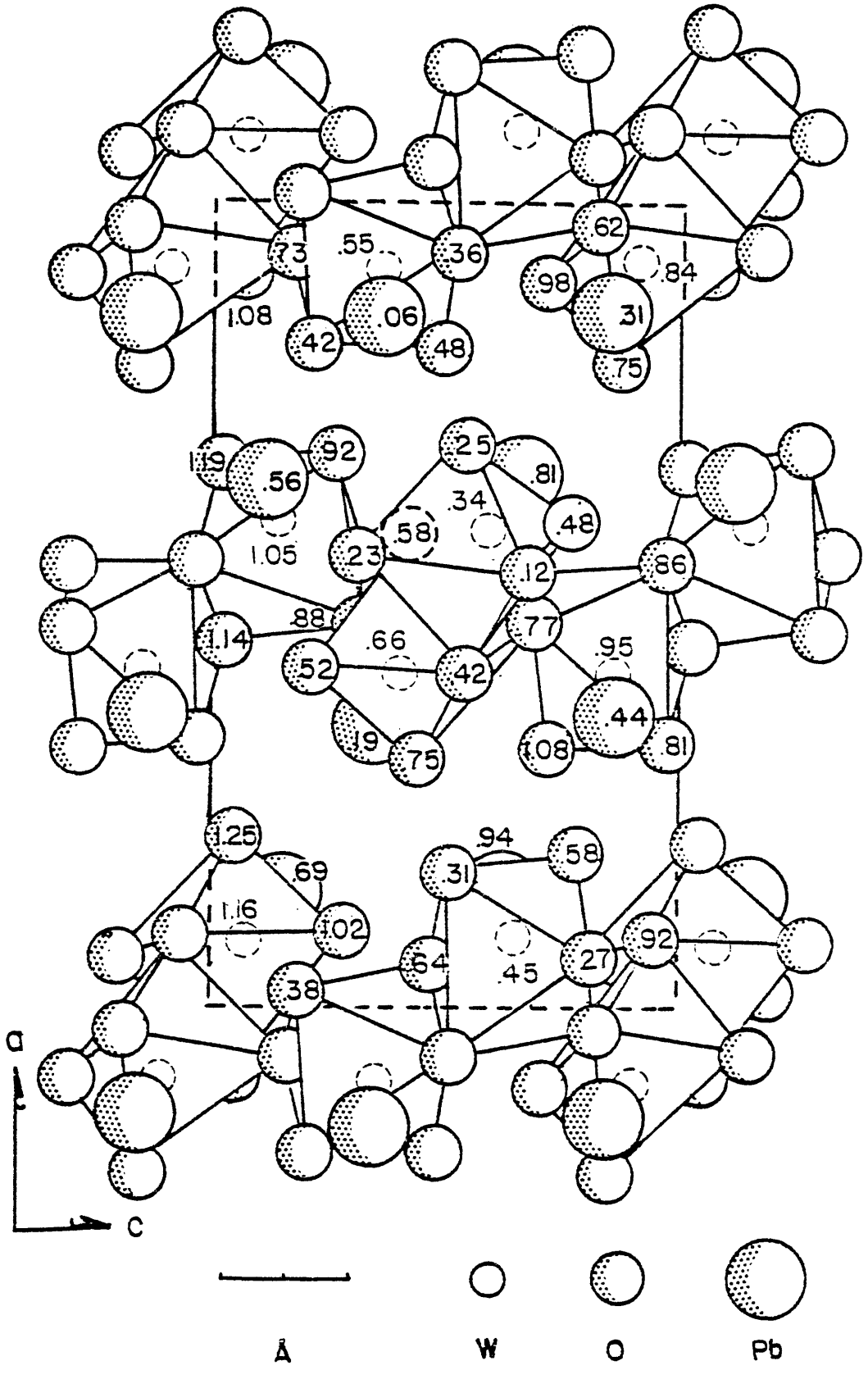

Figure 15. $PbWO_4$-III structure, {010} projection, from Richter, et al. 1976. Numbers represent y coordinates of the atoms.

Table 5. Bond lengths and angles of $PbWO_4$-III (from Richter et al. 1976).

W - O Bond Lengths

	W_1		W_2
01	1.79	02	1.81
04	1.81	03	1.91
07	1.83	05	1.88
05	2.10	06	1.76
08	2.03	03	2.17
08	2.16	07	2.26
Average	1.95 Å	Average	1.97 Å

O - W - O Angles Around W_1

	04	07	05	08	08
01	104	101	165	87	90
04		98	85	105	166
07			89	154	83
05				80	80
08					72

O - W - O Angles Around W_2

	03	05	06	03	07
02	98	98	100	162	82
03		152	101	76	81
05			98	82	80
06				97	177
03					81

Pb - O Bond Lengths

	Pb1		Pb2
01	2.59	01	2.67
02	2.88	02	2.79
03	3.65	02	2.49
04	3.28*	03	2.63
04	2.76	04	2.61
05	2.57	05	2.99
06	2.75	06	2.75
07	2.70	08	2.44
08	2.43		
Average	2.67 Å	Average	2.67 Å

*Not included in average.

this direction, the raspite structure also consists of slabs of tungsten-oxygen polyhedra perpendicular to the long axis of the unit cell. As mentioned earlier, the coordination of oxygen around tungsten is almost octahedral, although the sixth bond length is considerably too long at 2.76 Å. It is probable that if the oxygen positions in raspite had refined better, the coordination around tungsten would have turned out to be octahedral. Unlike $PbWO_4$-III, the tungsten-oxygen "octahedra" in raspite are bound together firmly in one direction only, forming chains parallel to the b axis. The individual chains are bonded to each other by the weak Pb-O bonds extending across the cleavage. The lead atoms in $PbWO_4$-III are all surrounded by eight oxygen atoms at an average distance of 2.67 Å. The higher density of this phase with respect to the other two lead tungstates is easily accounted for in terms of the lower coordination of oxygen around lead in raspite, and the considerably longer Pb-O bonds found in stolzite. Coordination, bond lengths and density of these three polymorphs are summarized in table 6.

Table 6. Comparison of density, coordination and bond lengths for the three $PbWO_4$ polymorphs.

	Density (g/cm^3)	Coord. Around W	Avg W-O Bond Length (Å)	Coord. Around Pb	Avg Pb-O Bond Length (Å)
Stolzite $V=355.4Å^3$ $Z=4$ $I4_1/a$	7.9-8.3	4	1.78	8 (4)	2.90 (2.59)
Raspite $V=358.4Å^3$ $Z=4$ $P2_1/c$	8.46	5	1.9	7 (5)	2.64 (2.44)
$PbWO_4$-III $V=658.1Å^3$ $Z=8$ $P2_1/n$	9.19	6	1.95	8	2.67

CONCLUSIONS

The crystal structure determined for raspite during the course of this study may be considered correct with a few reservations. The heavy atoms are undoubtedly correctly located. The general arrangement of the oxygen atoms is also probably correct. Some of the calculated bond lengths deviate significantly from expected values and thus cast doubt on the validity of specific oxygen positions. These doubts could be cleared by refining the structure using more sophisticated absorption corrections and anomalous dispersion corrections. In any event, the proposed structure accounts in detail for the physical properties displayed by raspite. The heavy atom positions determined by Shaw and Claringbull but never published, are the same as those determined here but with the origin shifted by (1/2, 1/2, 1/2). The Shaw and Claringbull study, using film data and Patterson projections, located the heavy atoms with less precision than those determined here. The present study also successfully located oxygen positions. As a result, it was possible to distinguish between the lead and tungsten atoms.

The raspite structure, when compared to those of the two other polymorphs of $PbWO_4$, shows similarity to both. The most striking similarities lie between raspite and stolzite, the raspite structure being a distorted version of

stolzite. The atom positions, with the exception of the *y* coordinates of the "middle" tetrahedral pair are entirely analogous between the two. The similarities between raspite and $PbWO_4$-III become apparent when the raspite structure is viewed projected on {100}. The nearly octahedral coordination of tungsten in raspite and the edge sharing of these octahedra to form sheets perpendicular to the long dimension of the unit cell are very like the structure of $PbWO_4$-III. Thus it seems that the raspite structure is intermediate between that of the two other polymorphs.

Because raspite has never been synthesized, it is difficult to speculate on the relation, if any, between raspite and stolzite. It is not clear from hand specimens containing both minerals whether or not the two crystallized simultaneously. It seems unlikely that two minerals of the same composition but having different albeit very similar structures could form under the same physical conditions. It may be that the traces of manganese and iron reported in the published raspite analysis (Dana, 1951) are real and play an integral part in the crystallization of raspite. The inability to synthesize raspite could then be a result of working with a pure Pb-W-O system when what was needed was to dope the system with a little manganese and iron. If this were true, the two minerals could have formed under similar pressure and temperature conditions which seems

reasonable considering the similarity of the two structures. The fact that two different minerals did form would then reflect differing metal concentrations in the fluids from which the minerals crystallized.

APPENDIX

RASPITE REFLECTION DATA

H	K	L	F(OBS)	F(CALC)
0	0	2	465.73	426.88
0	0	4	1594.18	-1640.87
0	0	6	103.91	82.51
0	0	8	504.64	-435.90
0	0	10	785.81	-676.12
0	0	12	827.07	670.60
0	0	14	937.76	652.26
0	1	-12	231.50	-222.93
0	1	-4	1358.67	-1676.39
0	1	-3	406.76	-414.76
0	1	1	319.98	327.85
0	1	2	191.95	-133.91
0	1	5	199.85	154.03
0	1	6	888.40	833.23
0	1	7	433.39	433.04
0	1	8	1527.30	-1332.45
0	1	9	101.93	-80.02
0	1	10	853.61	-727.96
0	1	11	74.50	-69.95
0	1	13	141.97	123.00
0	1	14	27.31	8.35
0	1	15	23.35	-14.96
0	2	-14	555.21	-482.17
0	2	-13	87.40	-68.51
0	2	-12	493.93	-498.44
0	2	-11	247.89	-244.82
0	2	-10	326.93	369.32
0	2	-9	382.02	425.51
0	2	-5	728.75	-733.36
0	2	-4	1228.59	1150.51
0	2	-3	335.42	237.76
0	2	0	1882.42	-2014.24
0	2	1	640.16	-656.03
0	2	2	235.77	-233.49
0	2	6	321.29	332.54
0	2	7	137.20	-143.24
0	2	8	409.54	369.18
0	3	-13	250.75	-234.09
0	3	-12	18.79	-15.67
0	3	-11	205.80	220.21
0	3	-10	441.18	-472.82
0	3	-9	270.51	285.90
0	3	-8	670.49	-706.43

H	K	L	F(OBS)	F(CALC)
0	3	-7	510.15	-538.19
0	3	1	445.60	-459.67
0	3	2	280.20	-305.20
0	3	3	727.61	799.79
0	3	4	1065.09	-1172.73
0	3	5	52.09	22.82
0	3	6	406.94	-445.59
0	4	-11	288.84	283.01
0	4	-9	302.35	-295.72
0	4	-8	343.03	-305.53
0	4	-5	556.96	558.00
0	4	-3	231.58	-242.15
0	4	-2	384.22	424.00
0	4	-1	541.88	-578.84
0	4	0	733.21	761.35
0	4	4	258.51	-263.19
0	4	6	493.22	-512.61
0	4	7	148.78	145.04
0	4	10	55.55	18.23
0	5	-7	374.01	323.55
0	5	-6	19.51	-23.14
0	5	-5	32.03	-6.63
0	5	-4	370.57	-363.49
0	5	-3	398.62	-400.03
0	5	-2	435.72	-456.95
0	5	1	274.79	274.64
0	5	8	225.08	-195.55
1	0	-14	77.97	-83.46
1	0	-12	607.03	-661.71
1	0	-10	58.23	-13.52
1	0	-8	1535.18	1892.81
1	0	-6	567.04	536.46
1	0	-4	1739.17	-1671.95
1	0	-2	580.65	-430.63
1	0	0	690.73	-448.37
1	0	2	1587.71	-1333.89
1	0	4	1079.97	1014.75
1	0	6	1597.56	1901.82
1	0	8	233.94	-285.63
1	0	10	813.65	-768.92
1	0	12	70.18	14.40
1	0	14	156.18	-104.31
1	1	-15	94.68	117.29
1	1	-14	281.67	-234.81
1	1	-13	20.71	9.48
1	1	-12	773.02	-837.44
1	1	-11	228.85	-280.09
1	1	-10	47.76	21.88
1	1	-9	98.58	106.88

H	K	L	F(OBS)	F(CALC)
1	1	-8	146.01	164.42
1	1	-7	114.46	87.23
1	1	-6	181.03	-227.00
1	1	-5	627.95	-620.84
1	1	-4	1590.29	1665.74
1	1	-3	124.23	-6.55
1	1	-2	1686.71	1387.26
1	1	-1	707.99	488.94
1	1	0	2430.33	-2147.48
1	1	1	307.75	-200.84
1	1	2	1531.74	-1457.53
1	1	3	97.60	-116.82
1	1	4	663.18	717.63
1	1	5	327.55	353.78
1	1	6	62.57	46.02
1	1	7	97.43	39.49
1	1	8	268.68	252.43
1	1	9	260.55	-222.54
1	1	10	1040.51	927.14
1	1	11	70.70	61.44
1	1	12	56.33	-36.11
1	1	13	158.38	107.81
1	1	14	842.72	-598.05
1	2	-15	104.69	82.74
1	2	-14	88.48	87.08
1	2	-13	269.71	-234.49
1	2	-12	407.09	393.96
1	2	-11	22.17	-10.92
1	2	-10	119.57	-132.23
1	2	-9	336.23	394.87
1	2	-8	1119.79	-1378.26
1	2	-7	267.78	-291.57
1	2	-6	424.03	-470.25
1	2	-5	389.93	-391.03
1	2	-4	1065.19	1116.22
1	2	-3	926.51	845.59
1	2	-2	544.68	424.69
1	2	-1	277.44	197.15
1	2	0	354.43	324.29
1	2	1	727.88	-767.02
1	2	2	659.40	707.50
1	2	3	414.90	485.04
1	2	4	803.76	-951.83
1	2	5	354.02	389.01
1	2	6	1302.55	-1340.16
1	2	7	552.50	-555.30
1	2	8	357.97	292.48
1	2	9	22.95	25.04
1	2	10	785.61	650.10

H	K	L	F(OBS)	F(CALC)
1	2	11	354,91	302.68
1	2	12	168,26	145.19
1	2	13	172,74	-125.35
1	3	-13	69,17	-54.77
1	3	-12	588,08	527.60
1	3	-11	382,01	381.74
1	3	-10	223,67	253.30
1	3	-9	244,82	-263.98
1	3	-8	23,33	0.03
1	3	-7	414,04	-454.95
1	3	-6	173,30	-230.80
1	3	-5	567,39	630.24
1	3	-4	1003,53	-978.05
1	3	-3	97,20	60.74
1	3	-2	558,72	-568.60
1	3	-1	711,81	-821.25
1	3	0	840,27	956.97
1	3	1	350,63	375.07
1	3	2	890,48	1022.87
1	3	3	532,91	531.19
1	3	4	130,34	104.44
1	3	5	559,97	-526.99
1	3	6	203,69	-146.01
1	3	7	119,44	-85.73
1	3	8	376,07	-316.08
1	3	9	540,19	416.40
1	3	10	608,33	-448.79
1	3	11	182,17	-117.11
1	3	12	49,32	22.88
1	4	-11	77,59	-64,69
1	4	-10	193,78	175.87
1	4	-9	389,77	-385.09
1	4	-8	504,60	532.78
1	4	-7	349,55	363.10
1	4	-6	317,49	317.97
1	4	-5	321,84	338.59
1	4	-4	305,29	-317.58
1	4	-3	492,89	-551.74
1	4	-2	509,82	-583.72
1	4	-1	140,24	139,39
1	4	0	403,87	-463.94
1	4	1	564,82	629.62
1	4	2	87,78	-47.38
1	4	3	406,02	-399.10
1	4	4	622,46	562.14
1	4	5	315,82	-280.25
1	4	6	638,88	547.33
1	4	7	530,17	434.99
1	4	8	44,35	-0.27

H	K	L	F(OBS)	F(CALC)
1	4	9	19,36	-11,91
1	4	10	351,54	-267,88
1	5	-8	18,04	-4,37
1	5	-7	292,72	258,26
1	5	-6	423,38	416,76
1	5	-5	312,90	-318,91
1	5	-4	392,61	388,31
1	5	-3	125,44	-99,80
1	5	-2	76,91	58,32
1	5	-1	452,62	453,62
1	5	0	235,25	-208,00
1	5	1	155,50	-171,52
1	5	2	424,91	-425,76
1	5	3	354,12	-337,93
1	5	4	280,43	-262,05
1	5	5	366,73	303,59
1	5	6	288,57	240,71
1	5	7	101,94	70,60
2	0	-16	612,70	559,10
2	0	-14	265,26	287,20
2	0	-12	565,13	-610,04
2	0	-10	267,36	-298,03
2	0	-8	215,01	-201,87
2	0	-6	943,97	-968,26
2	0	-4	733,29	643,78
2	0	-2	2431,64	2158,89
2	0	0	581,33	-413,66
2	0	2	1868,46	-1686,73
2	0	4	159,36	-62,78
2	0	6	264,45	-223,50
2	0	8	315,13	-356,42
2	0	10	629,11	724,10
2	0	12	470,30	455,45
2	1	-15	95,05	83,09
2	1	-14	87,65	-73,17
2	1	-13	165,21	-137,51
2	1	-12	545,65	588,42
2	1	-11	101,72	-111,89
2	1	-10	696,53	779,61
2	1	-9	259,61	254,70
2	1	-8	1098,46	-1230,87
2	1	-7	91,67	-15,01
2	1	-6	1362,50	-1439,47
2	1	-5	340,77	-361,16
2	1	-4	722,64	664,31
2	1	-3	365,55	282,73
2	1	-2	294,72	192,93
2	1	-1	247,08	202,83
2	1	0	213,06	124,89

H	K	L	F(OBS)	F(CALC)
2	1	1	770.47	-648.65
2	1	2	1719.12	1649.00
2	1	3	166.01	-111.58
2	1	4	210.23	177.83
2	1	5	282.13	250.89
2	1	6	1305.75	-1552.48
2	1	7	240.57	-272.31
2	1	8	384.94	-451.74
2	1	9	96.17	-112.79
2	1	10	378.19	379.29
2	1	11	177.38	171.55
2	1	12	82.93	76.19
2	2	-15	112.44	-122.00
2	2	-14	241.87	-219.02
2	2	-13	193.31	-184.54
2	2	-12	466.08	498.36
2	2	-11	273.26	333.97
2	2	-10	322.74	340.26
2	2	-9	67.45	23.40
2	2	-8	142.18	166.90
2	2	-7	474.81	-514.55
2	2	-6	499.63	511.23
2	2	-5	336.73	362.47
2	2	-4	901.99	-838.67
2	2	-3	363.53	303.15
2	2	-2	1843.93	-1800.08
2	2	-1	773.06	-725.11
2	2	0	237.99	188.48
2	2	1	102.93	-53.29
2	2	2	1153.60	1165.40
2	2	3	465.04	493.88
2	2	4	223.75	221.00
2	2	5	185.09	-217.32
2	2	6	173.02	198.87
2	2	7	177.31	-194.70
2	2	8	113.48	76.41
2	2	9	267.77	290.60
2	2	10	688.26	-643.29
2	2	11	75.73	48.41
2	2	12	492.92	-391.50
2	3	-13	237.55	208.79
2	3	-12	434.51	-440.38
2	3	-11	108.93	136.52
2	3	-10	345.63	-369.44
2	3	-9	458.46	-485.00
2	3	-8	467.48	499.80
2	3	-7	86.90	121.04
2	3	-6	719.52	781.94
2	3	-5	577.11	589.07

H	K	L	F(OBS)	F(CALC)
2	3	-4	59,09	50,97
2	3	-3	555,00	-532,52
2	3	-2	313,34	-269,29
2	3	-1	363,21	-362,52
2	3	0	445,63	-424,38
2	3	1	671,64	695,45
2	3	2	724,31	-763,73
2	3	3	164,04	-164,11
2	3	4	23,77	-28,42
2	3	5	515,40	-560,80
2	3	6	728,34	795,73
2	3	7	318,13	322,93
2	3	8	366,87	357,81
2	3	9	198,87	151,45
2	3	10	168,19	-139,37
2	4	-11	308,39	-289,25
2	4	-10	340,40	-334,99
2	4	-9	37,00	-33,51
2	4	-8	263,61	-293,18
2	4	-7	421,53	449,01
2	4	-6	112,77	-68,19
2	4	-5	299,40	-323,76
2	4	-4	507,08	493,97
2	4	-3	460,29	-434,52
2	4	-2	717,40	661,52
2	4	-1	518,71	502,22
2	4	0	59,89	18,67
2	4	1	84,93	44,25
2	4	2	481,20	-486,44
2	4	3	513,25	-516,71
2	4	4	423,54	-456,63
2	4	5	235,73	239,01
2	4	6	194,73	-192,33
2	4	7	326,59	278,50
2	4	8	169,01	148,93
2	5	-8	185,12	-175,86
2	5	-7	87,79	-85,38
2	5	-6	424,46	-373,33
2	5	-5	380,03	-328,47
2	5	-4	341,16	-318,00
2	5	-3	315,66	276,25
2	5	-2	245,54	217,16
2	5	-1	141,48	133,97
2	5	0	515,20	515,84
2	5	1	379,57	-370,85
2	5	2	237,06	225,31
2	5	3	100,41	95,19
2	5	4	111,68	-101,64
2	5	5	298,15	273,19

H	K	L	F(OBS)	F(CALC)
3	0	-14	273,80	-296,31
3	0	-12	270,52	251,43
3	0	-10	1169,08	1290,17
3	0	-8	104,47	-105,73
3	0	-6	1273,50	-1321,04
3	0	-4	144,00	184,94
3	0	-2	135,25	-24,83
3	0	0	616,41	-560,69
3	0	2	1343,27	1313,63
3	0	4	1033,48	1087,27
3	0	6	764,08	-812,23
3	0	8	598,18	-666,62
3	0	10	73,73	42,10
3	1	-15	28,27	32,04
3	1	-14	547,46	-541,03
3	1	-13	109,90	-94,71
3	1	-12	199,33	160,01
3	1	-11	139,34	160,62
3	1	-10	228,06	234,47
3	1	-9	234,69	241,36
3	1	-8	98,54	88,68
3	1	-7	234,73	-236,06
3	1	-6	1046,09	1066,65
3	1	-5	26,57	-13,66
3	1	-4	416,74	394,83
3	1	-3	413,84	363,77
3	1	-2	1766,40	-1736,70
3	1	-1	258,80	-215,05
3	1	0	987,77	-936,14
3	1	1	208,23	-177,28
3	1	2	747,84	710,49
3	1	3	313,48	334,01
3	1	4	207,19	226,57
3	1	5	43,42	39,37
3	1	6	200,09	220,73
3	1	7	163,70	-163,83
3	1	8	527,61	602,70
3	1	9	58,17	77,55
3	1	10	201,26	-218,81
3	1	11	56,22	46,03
3	2	-14	209,82	194,11
3	2	-13	125,51	125,86
3	2	-12	241,91	-256,72
3	2	-11	219,96	227,15
3	2	-10	831,66	-890,85
3	2	-9	346,01	-374,03
3	2	-8	73,12	60,12
3	2	-7	87,96	-143,85
3	2	-6	978,26	1039,78

H	K	L	F(OBS)	F(CALC)
3	2	-5	442.02	465.02
3	2	-4	363.57	354.14
3	2	-3	250.19	-212.06
3	2	-2	223.55	217.35
3	2	-1	415.15	-417.06
3	2	0	275.82	269.31
3	2	1	435.06	451.73
3	2	2	896.03	-939.27
3	2	3	157.03	154.72
3	2	4	819.02	-869.56
3	2	5	409.23	-435.13
3	2	6	445.35	483.64
3	2	7	66.45	58.75
3	2	8	478.92	543.55
3	2	9	174.49	179.82
3	2	10	33.80	32.75
3	3	-13	269.39	265.33
3	3	-12	40.71	21.75
3	3	-11	171.91	-167.05
3	3	-10	167.28	-157.25
3	3	-9	204.33	-229.73
3	3	-8	225.83	-219.77
3	3	-7	479.83	501.42
3	3	-6	608.74	-616.98
3	3	-5	44.45	16.88
3	3	-4	110.86	-91.26
3	3	-3	616.44	-582.52
3	3	-2	957.54	936.93
3	3	-1	355.85	362.10
3	3	0	486.51	487.10
3	3	1	362.36	360.15
3	3	2	307.70	-302.22
3	3	3	450.12	-465.07
3	3	4	269.35	-295.37
3	3	5	20.64	10.04
3	3	6	342.61	-355.99
3	3	7	327.46	335.11
3	3	8	276.85	-275.13
3	3	9	166.34	-162.02
3	4	-11	236.81	-230.47
3	4	-10	378.29	354.77
3	4	-9	280.62	279.93
3	4	-8	81.48	91.28
3	4	-7	118.68	122.30
3	4	-6	405.19	-352.50
3	4	-5	518.34	-494.05
3	4	-4	479.37	-471.76
3	4	-3	155.73	140.34
3	4	-2	165.59	-170.09

H	K	L	F(OBS)	F(CALC)
3	4	-1	418,61	392,92
3	4	0	205,77	211,34
3	4	1	406,41	-388,88
3	4	2	474,68	466,62
3	4	3	142,14	-138,38
3	4	4	357,88	338,04
3	4	5	363,40	353,38
3	4	6	154,24	-129,88
3	5	-6	243,95	214,51
3	5	-5	46,83	25,34
3	5	-4	111,76	-121,39
3	5	-3	371,40	333,53
3	5	-2	352,08	-321,01
3	5	-1	218,74	-179,96
3	5	0	388,29	-340,04
3	5	1	219,56	-194,19
3	5	2	136,69	-114,68
4	0	-14	610,19	-529,21
4	0	-12	94,00	-93,95
4	0	-10	75,77	83,87
4	0	-8	349,82	-322,17
4	0	-6	826,27	801,34
4	0	-4	1182,69	1200,09
4	0	-2	772,36	-752,71
4	0	0	1088,68	-1111,04
4	0	2	170,27	144,41
4	0	4	42,84	39,69
4	0	6	65,57	17,48
4	0	8	601,48	654,07
4	1	-14	402,64	361,28
4	1	-13	37,15	-18,80
4	1	-12	239,30	237,82
4	1	-11	142,70	115,91
4	1	-10	799,10	-842,27
4	1	-9	110,07	-148,53
4	1	-8	607,53	-640,21
4	1	-7	102,03	-138,24
4	1	-6	563,21	579,13
4	1	-5	235,48	225,81
4	1	-4	291,74	249,82
4	1	-3	93,52	75,09
4	1	-2	177,28	181,83
4	1	-1	141,08	-130,24
4	1	0	839,46	865,53
4	1	1	140,22	145,04
4	1	2	254,23	-245,17
4	1	3	170,98	167,91
4	1	4	995,64	-1088,84
4	1	5	94,93	-121,02

H	K	L	F(OBS)	F(CALC)
4	1	6	74,18	-78,63
4	1	7	75,88	-39,49
4	1	8	363,68	389,57
4	1	9	108,08	105,12
4	2	-14	413,00	361,13
4	2	-13	216,01	192,27
4	2	-12	184,41	170,74
4	2	-11	22,63	1,34
4	2	-10	35,22	43,44
4	2	-9	276,43	-299,14
4	2	-8	178,95	168,26
4	2	-7	282,44	301,60
4	2	-6	592,37	-630,43
4	2	-5	285,05	314,74
4	2	-4	864,94	-878,98
4	2	-3	448,01	-448,23
4	2	-2	520,40	501,05
4	2	-1	23,17	40,83
4	2	0	818,50	851,19
4	2	1	403,41	402,91
4	2	2	81,47	61,66
4	2	3	276,22	-283,04
4	2	4	49,10	51,90
4	2	5	155,44	-159,04
4	2	6	35,22	-43,52
4	2	7	230,12	257,65
4	2	8	429,83	-453,48
4	3	-12	79,63	-41,46
4	3	-11	295,17	-291,72
4	3	-10	522,02	503,57
4	3	-9	151,64	155,17
4	3	-8	410,72	423,77
4	3	-7	281,39	274,06
4	3	-6	201,48	-189,90
4	3	-5	365,24	-365,14
4	3	-4	295,60	-301,82
4	3	-3	21,71	-51,69
4	3	-2	326,08	-310,07
4	3	-1	456,28	447,68
4	3	0	366,82	-343,70
4	3	1	158,53	-155,97
4	3	2	250,02	258,98
4	3	3	264,20	-265,46
4	3	4	631,59	645,87
4	3	5	262,70	269,23
4	3	6	151,80	152,39
4	4	-9	305,90	282,84
4	4	-8	148,82	115,41
4	4	-7	230,28	-201,62

H	K	L	F(OBS)	F(CALC)
4	4	-6	397,35	371.35
4	4	-5	160,05	-141.82
4	4	-4	363,40	324.73
4	4	-3	448,12	417.86
4	4	-2	149,01	-135.15
4	4	-1	19,71	-20.00
4	4	0	445,63	-397.87
4	4	1	355,24	-330.77
4	4	2	257,53	-242.66
4	4	3	208,98	196.72
5	0	-12	607,69	504.53
5	0	-10	333,46	-313.61
5	0	-8	794,03	-827.48
5	0	-6	21,88	-27.41
5	0	-4	83,77	65.03
5	0	-2	122,54	-120.24
5	0	0	732,70	742.40
5	0	2	473,15	471.08
5	0	4	632,90	-667.00
5	0	6	385,38	-420.19
5	1	-13	59,72	54.12
5	1	-12	164,25	136,50
5	1	-11	19,10	38,66
5	1	-10	59,42	35.63
5	1	-9	141,41	-152.86
5	1	-8	499,81	518.46
5	1	-7	30,99	33.19
5	1	-6	46,41	-95.36
5	1	-5	151.01	156.86
5	1	-4	996,40	-1032.84
5	1	-3	173,30	-197.04
5	1	-2	149,64	-157.02
5	1	-1	116,57	-140.02
5	1	0	580,49	589,96
5	1	1	146,60	140,49
5	1	2	119,46	129,53
5	1	3	56,28	-67.98
5	1	4	158,95	159,02
5	1	5	121,54	-116,75
5	1	6	253,39	243,72
5	2	-12	450,41	-414,76
5	2	-11	202,25	-188,09
5	2	-10	200,44	184.35
5	2	-9	19,63	-13,88
5	2	-8	542,16	540,37
5	2	-7	282,24	255,16
5	2	-6	38,62	16,53
5	2	-5	168,99	-174,76
5	2	-4	60,48	-60,07

H	K	L	F(OBS)	F(CALC)
5	2	-3	212.56	-201.67
5	2	-2	38.22	-46.33
5	2	-1	269.92	261.19
5	2	0	587.48	-595.28
5	2	1	58.65	44.69
5	2	2	296.26	-310.01
5	2	3	207.99	-202.50
5	2	4	481.02	471.71
5	3	-10	180.97	-182.38
5	3	-9	276.72	262.12
5	3	-8	239.57	-222.76
5	3	-7	98.80	-82.67
5	3	-6	110.10	133.62
5	3	-5	306.41	-311.83
5	3	-4	638.09	597.18
5	3	-3	259.37	245.16
5	3	-2	253.27	232.91
5	3	-1	106.35	125.42
5	3	0	321.50	-290.11
5	3	1	323.38	-322.95
5	3	2	230.15	-230.34
6	0	-10	80.85	-59.41
6	0	-8	434.88	471.88
6	0	-6	417.57	419.66
6	0	-4	565.77	-558.31
6	0	-2	495.78	-478.64
6	0	0	166.29	141.86
6	0	2	27.56	9.71
6	1	-10	161.88	-167.64
6	1	-9	77.73	-74.59
6	1	-8	412.58	395.53
6	1	-7	122.68	114.69
6	1	-6	143.82	144.67
6	1	-5	20.43	-21.57
6	1	-4	79.82	48.86
6	1	-3	162.33	-138.70
6	1	-2	290.97	275.16
6	1	-1	88.23	88.04
6	1	0	308.81	-298.36
6	1	1	60.87	73.09
6	2	-8	349.51	-324.70
6	2	-7	44.51	35.89
6	2	-6	298.35	-264.11
6	2	-5	211.32	-202.42
6	2	-4	454.19	417.97
6	2	-3	70.70	61.21
6	2	-2	423.36	422.24
6	2	-1	163.37	164.20

REFERENCES

Ahmed, F. R., Hall, S. R., Pippy, M. E., Saunderson, C. P., 1967, NRC Crystallographic Programs for the IBM/360 System.

Bragg, L., Claringbull, G. F., Taylor, W. H., 1965, The Crystalline State, vol. IV, Crystal Structures of Minerals, Cornell University Press.

Buerger, M. J., 1959, Vector Space, John Wiley and Sons, Inc.

_____, 1960, Crystal-Structure Analysis, John Wiley and Sons, Inc.

Busing, W. R., Martin, K. O., Levy, H. A., 1962, OAK RIDGE FORTRAN LEAST SQUARES, in ORNL - TM - 305.

_____, Levy, H. A., 1957, Journal of Chemical Physics, vol. 26, no. 3, p. 563, Neutron Diffraction Study of Calcium Hydroxide.

Corfield, P. W. R., Doedens, R. J., Ibers, J. A., 1967, Inorganic Chemistry, vol. 6, no. 2, pp. 197-204, Studies of Metal-Nitrogen Multiple Bonds, I.

Cromer, D. T., and Mann, J. B., 1968, Acta. Cryst., vol. A24, pp. 321-324.

Dana's System of Mineralogy, vol. II, Seventh Edition, 1951, John Wiley and Sons, Inc.

Hlawatsch, C., 1898, Zeit. fur Krist., vol. 29, pp. 130-139, Ueber Stolzit und Raspit von Brokenhill.

_____, 1899, Zeit. fur Krist., vol. 31, pp. 1-10, Krumme Flachen und Aetzerscheinungen am Stolzit. Element p. des Raspit.

_____, 1907, Zeit. fur Krist., vol. 42, pp. 587-595, Neue Messungen am Raspit von Brokenhill.

The International Tables for X-Ray Crystallography, Volumes I, II, and III, 1962, Kynoch Press.

Park, C. F., MacDiarmid, R. A., 1970, Second Edition, Ore Deposits, pp. 303-313, W. H. Freeman and Company.

Richter, P. W., Kruger, G. J., and Pistorius, C. W. F. T., 1976, Acta. Cryst., vol. B32, pp. 928-929, $PbWO_4$-III (A High Pressure Form).

Shaw, R., and Claringbull, G. F., 1955, Amer. Min., vol. 40, p. 933, X-Ray Study of Raspite (Monoclinic $PbWO_4$).

Stout, G. H., and Jensen, L. H., 1968, X-Ray Structure Determination, A Practical Guide, The Macmillan Company.

Weitzel, H., 1976, Zeit. fur Krist., vol. 144, p. 238-258, Kristallstrucktur verfeinerung von Wolframiten und Columbiten.

Wyckoff, R. W. G., 1965, Crystal Structures, vol. 3, Interscience Publishers, John Wiley and Sons.